Alkali enhanced common reed properties for bio - composite applications

Novenya Gunathilaka

Degree Thesis
Mechanical and Sustainable Engineering
2025

Degree Thesis

Novenya Gunathilaka
Arcada University of Applied Sciences: Mechanical and Sustainable Engineering, 2025
Identification Number: 047920376

Abstract:

This thesis investigates the effect of alkali treatment using sodium hydroxide on the structural and chemical properties of common reed for application in bio-composites. The aim was to evaluate how NaOH treatment influences reed fiber performance in composite materials and to assess compatibility with three thermoplastic polymers: PP, PLA, and HDPE. The study employed a fixed NaOH concentration (4.5%) and treatment duration (five hours) to process reed fibers, which were subsequently incorporated at 20 wt% into the polymer matrices. Composite formulations were processed via micro-compounding and injection molding. Characterization was conducted using FTIR to identify chemical changes, optical microscopy for structural analysis, and Melt Flow Index testing to evaluate flow behavior. FTIR results confirmed the successful removal of hemicellulose and lignin, as evidenced by the disappearance of the C=O peak at 1730 cm^{-1} and sharpening of cellulose-associated peaks, indicating increased crystallinity. Microscopy revealed enhanced fiber dispersion, reduced interfacial gaps, and improved matrix adhesion in treated composites. These effects were most prominent in PP and PLA composites. However, MFI testing yielded inconsistent results due to equipment limitations and moisture-related issues, with only HDPE-based composites providing valid flow data. The findings affirm that NaOH treatment improves reed fiber integration and structural characteristics in bio-composites but highlight challenges in optimizing treatment conditions and processing parameters. Future work should explore varied treatment settings and incorporate mechanical testing to better quantify composite performance.

Keywords:

Common reed, Phragmites australis, Alkali treatment, Bio-composites, FTIR Analysis, Optical Microscopy, Melt flow Index

Contents

List of Figures

Abbreviations

ASTM	American Society for Testing and Materials
ATR	Attenuated Total Reflectance
BF	Bright Field
DF	Dark Field
DSC	Differential Scanning Calorimetry
FTIR	Fourier Transform Infrared
HDPE	High density polyethelene
HWE	Hot Water Extraction
ISO	International Organization for Standardization
MFI	Melt flow index
NaOH	Sodium hydroxide
PLA	Polylactic Acid
PP	Polypropelene
RL	Reflected Light
SEM	Scanning Electron Microscopy
TGA	Thermogravimetric Analysis
TL	Transmitted Light

1 Introduction

1.1 Background

Natural fibers are gaining more significance with the growing demand for sustainable materials since they can be used to replace traditional petroleum-based synthetic fibers. Common reed (*Phragmites australis*) is a valuable resource because of its worldwide availability and favorable properties (Huhta, 2009). Reed is a perennial aquatic grass growing on river banks and by the sea coast. Being one of the most extensively distributed plants, this tall, slender-stemmed plant is present in the temperate and tropical regions of Europe, Asia, and North America (The Lake Huron Centre for Coastal Conservation, 2006). Over the centuries, the common reed has been used by all cultures for various uses, such as roofing, thatching, handicrafts, and animal fodder (Huhta, 2009).

The role of natural fibers in bio-composites has changed significantly from earlier times to now. Traditionally, natural fibers such as grass, straw, and animal hair were used in simple applications such as reinforcing mud bricks. Natural fibers were mainly substituted by artificial materials in engineered composites during the 20th century. However, with the growth in the environment in recent decades, natural fiber composites have ranked high. Researchers have started modifying the mechanical properties of natural fibers, like strength and water resistance, to enable natural fibers to compete with synthetic fibers (Kabir et al., 2012). The development of biopolymers like Polylactic Acid and Polyhydroxyalkanoate has improved the strength and durability of these composites, and they are now emerging as an alternative to conventional synthetic plastics in a wide range of applications, from packaging to automotive parts (Madhavan Nampoothiri et al., 2010).

As science pushes beyond the present limitations, natural fiber-reinforced bio-composites will be commonplace in a vast number of industries, offering a cleaner, greener alternative to synthetic plastics and paving the way to a more sustainable future. Natural fibers such as hemp, flax, and wood fibers have been well-studied to be used in bio-composites. Common reed has been proposed as a good alternative because of its superior characteristics, like high cellulose content, low density, and mechanical strength (Wang et al., 2013a). As promising as it is, reed has not yet been well studied in the field of composite materials science (Abou-Zeid et al., 2015).

Due to the structural integrity of cellulose and corresponding natural constituents, like hemicellulose and lignin, that provide flexibility and binding characteristics to it, high cellulose content reed fibers (33–51%) are most appropriate for bio-composites (Abou-Zeid et al., 2015). Reed is an effective reinforcement for polymer matrices due to its highly fibrous nature, which imparts optimum weight, strength, and durability (Abou-Zeid et al., 2015). However, lignin and hemicellulose interfere with bonding, and reed fibers are hydrophilic, absorbing water and making the fiber-matrix bond loose. These problems are alleviated by the elimination of non-cellulosic components, improved surface roughness, and compatibilization between fiber and matrix by chemical treatment in the form of alkali treatment with NaOH (Kabir et al., 2012).

Aside from having excellent material properties, reed-based Bio-composites could adhere to the principles of the circular economy. Common reed is a green raw material since it is an annual renewable resource that can be typically harvested throughout the year, except for seasonal variations, such as winter or summer reed (Huhta, 2009). Moreover, the reed's capacity to retain nutrients and carbon, especially in wetland ecosystems, protects the environment. Industries can minimize their reliance on fossil fuel-based products, lower their carbon footprint, and promote the use of biodegradable products by using reed in the production of Bio-composite products (Başaran Kankılıç & Metin, 2020).

1.2 Objective of Thesis

1. To investigate the effects of NaOH treatment such as, structure, and appearance of reed fibers, with emphasis on the changes it causes in their properties.

2. To determine the optimal conditions for improving fiber performance and analyze the effects of NaOH treatment on the crystallinity of reed fibers using FT-IR spectroscopy.

3. To observe the surface characteristics and structural integrity of the bio-composites, using microscopy, in order to examine the effects of alkali treatment on their morphology.
4. To compare the quality of treated reed fibers for processing by analyzing their compatibility with different polymer matrices and performing MFI tests.

1.3 Structure of the Thesis

The foundation of this thesis is an extensive review of the literature that supports the textual analysis and findings expressed here. Along with university laboratory experimental activity, this study synthesises earlier efforts on reed and reed-based bio-composites. Including their chemical composition, structural properties, crystallinity, and processability, the literature review provides a thorough picture of the key features of reed fibers. Moreover, it looks at how reed fibers might be used in Bio-composite applications, underlining their possible sustainability.

From reliable databases, including ScienceDirect, ResearchGate, and MDPI, a varied collection of scholarly sources, including journal articles, books, and research papers was investigated to enable a comprehensive review of the subject. These materials gave vital new perspectives on the alkali treatment of reed fibers and their use in composite materials. The knowledge gained from these sources affected not only the experimental strategy used in this thesis but also provided the necessary background for comprehending the laboratory findings, hence producing a thorough and educated interpretation.

2 Litreature Review

2.1 Fibers and their types

Fibers are long, thread-like objects with a high length-to-diameter ratio. Their combination of mechanical strength, pliability, and lightness has made them extremely useful in many applications like textiles and construction of buildings. They are classified into three general categories: natural, synthetic, and manufactured (regenerated) fibers (Khan et al., 2023). Synthetic fibers like nylon and polyester are made from petroleum-based polymers. Regenerated cellulose fibers include viscose, which is chemically produced from natural cellulose (Khan et al., 2023). Natural fibers, directly come from biological sources, including minerals, animals, and plants. Plant-based natural fibers have attracted growing attention owing to their abundance, renewability, and compatibility with sustainable development concepts (Kabir et al., 2012).

Plant fibers are primarily made of lignocellulosic materials, and their structure and properties vary depending on their botanical origin. These variations influence their quality and suitability for different applications. They are typically categorized according to the part of the plant they come from: bast fibers e.g., flax, hemp, jute from stem phloem; leaf fibers e.g., sisal, pineapple from leaf vascular bundles; seed fibers e.g., cotton, coir covering seeds or fruits; and stalk, grass, and wood/root fibers from other parts of plants. Its anatomical origin defines a fiber's mechanical properties; thus, this botanical difference is essential. Bast fibers, generally having high tensile strength and flexibility, find application as structural reinforcements (Kabir et al., 2012). Seed and fruit fibers, being lighter and bulkier, would find greater application in areas like thermal insulation and cushioning (Li et al., 2021).

2.2 Plant Fibers

Plant fibers provide mechanical integrity and allow for the transport of nutrients via structural and physiological roles. The functionality of engineered materials, particularly composites, depends on their microstructure, chemical composition, and physical properties. These vary not only with fiber type but also with species and age of the plant. Flax and hemp contain highly cellulose and possess good mechanical properties among bast fibers. They possess high length, strength, and stiffness and are suitable for load-bearing Bio-composites (Amin et al., 2022). Though rough, leaf fibers like sisal are a source of high mechanical strength. A seed

fiber, cotton is valued for softness and purity and dominates the textile industry (Amin et al., 2022).

Grasses like bamboo and common reed have emerged as potential alternatives with their high growth rates and structural characteristics. Constituted silica-rich material with different micro fibril angles, reed has a sophisticated microstructure that adds to its mechanical and chemical resistance (El Shahawy & Heikal, 2018). While plant fibers benefit the environment such as low density, biodegradability, and renewability, their performance might be inconsistent owing to factors ranging from exposure to the environment to variation in plant components (El Shahawy & Heikal, 2018).

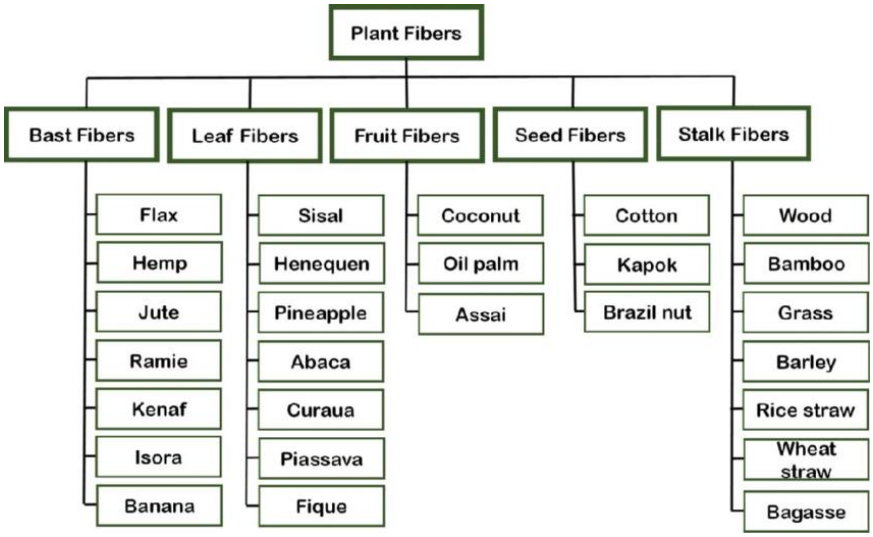

Figure 1 Plant Fiber Characterization (Güven et al., 2016)

2.2.1 Properties of Plant Fibers

Plant fibers' mechanical and physical properties control their performance in composite uses. Thus, their internal structure and composition dictate these properties. Among their most valuable benefits is that they have a high strength-to-weight ratio. Having tensile strengths over 600 MPa and Young's moduli of up to 70 GPa, fibers such as hemp and flax are comparable to low-grade glass fibers (Kabir et al., 2012).

Most plant fibers' hollow and cellular morphology provides improved thermal insulation and sound-absorbing qualities, making them appropriate for packaging and building materials. However, their hydrophilic character is highly undesirable.

2.2.2 Chemical composition of plant fibers

Plant fibers mainly comprise three biopolymers cellulose, hemicellulose, and lignin. Linear polysaccharide cellulose, comprising glucose units, creates micro fibrils to provide strength and stiffness to the fiber. Based on the plant species, plant fiber content ranges from 40% to 80%. A matrix surrounding cellulose micro fibrils, hemicellulose is a shorter, branched polysaccharide that creates flexibility. Less stable than cellulose, it is also more vulnerable to breakdown by bacteria.

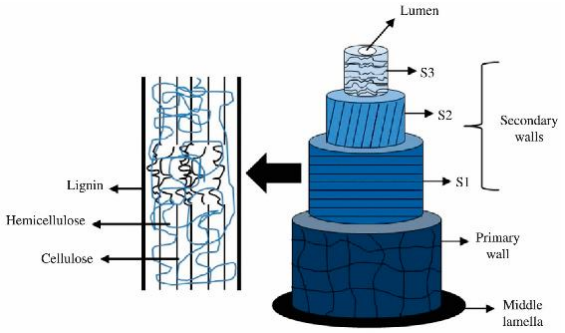

Figure 2 Structure of Natural Fibers (Lavorel et al., 2021)

An amorphous, aromatic polymer, lignin contributes thermal stability, ultraviolet resistance, and stiffness. It has longevity, but higher lignin content can reduce flexibility and cause processing to be more problematic. Mechanical performance is especially influenced by the hierarchical plant cell wall structure, notably the multi-layered secondary wall (especially the S2 layer). Other inorganic substances like silica are integrated into the fibers of particular species, thereby enhancing their quality value. Common reed, for instance, forms silica to strengthen its structural value and special chemical characteristics (Kabir et al., 2012).

2.3 Reed Fiber

2.3.1 Properties of reed

The intrinsic value of reed, influencing the durability and longevity of reed thatches to a large extent, is affected by various parameters, including the source of the reed, climatic factors, and cutting management practices. A study by Wöhler-Geske examined 214 reed bunches from 12 countries in Europe and Asia, including Germany, the Netherlands, Turkey, Romania, and China, and they were primarily harvested between 2009 and 2011. This long-duration study is a detailed examination of the morphological and chemical characteristics of reed, which reveals

deep insights into its suitability for use as a thatch and in other uses (Wöhler-Geske et al., 2016).

The morphological characteristics of a reed are decisive in determining the structural ability and general suitability of a reed for thatching. The mean culm diameter of the reed varies between 2.4 mm and 7.7 mm, and the wall thickness varied from 0.2 mm to 0.8 mm. The mean bunch lengths are approximately 184 cm, whereas conicity values between 0.4 and 1.1, which are a measure of the degree of tapering. The reed density, which is an important parameter to determine its sensitivity to environmental degradation, has been computed through two different methods with values ranging from 320 kg/m³ to 788 kg/m³ (Wöhler-Geske et al., 2016). The results attest to extensive variability in the reed's properties concerning environmental conditions, harvesting period, and test procedure. The extensive range in these morphological characters underlines the difficulties of standardizing reed quality for construction purposes, indicating the necessity for more focused work on the ideal conditions for reed cutting. The chemical composition of the reed is most important in determining the reed's durability as a material for thatching.

Crude cellulose is the principal dry matter component of reed, accounting for approximately 51.5%, while hemicellulose accounts for 26.9% and lignin for 11.9% (Wöhler-Geske et al., 2016). The content of crude ash varied between 0.69% and 8.07%, with elevated concentrations of calcium usually attributed to contamination from other vegetation. Nitrogen concentration ranged from 0.05% to 0.67%, and the C/N ratio also had a comprehensive range from 76 to 963 with a mean of 290. The chemical characteristics are closely associated with the resistance of reed against rot and microbial degradation, where high lignin content is reported to be associated with increased durability. The variability of such chemical elements, conditioned by soil fertility, climate, and processing techniques, confirms the reed quality's complexity (Wöhler-Geske et al., 2016). The chemical properties of reed make it highly suitable for use in composite materials. The high cellulose content provides excellent mechanical strength and rigidity, which is critical for reinforcing polymer matrices in bio-composites. Hemicellulose contributes to flexibility, which can help absorb stress and prevent brittleness in the final product. Lignin enhances thermal stability and UV resistance, improving the composite’s durability in outdoor or high-temperature applications. Additionally, the presence of ash and minerals like calcium can influence the composite’s fire resistance and thermal behavior. These

chemical traits, when balanced correctly through treatment or processing, enable reed fibers to improve the strength, durability, and functionality of sustainable composite materials.

2.3.2 Suitability of reed

Reed has shown great promise as a sustainable material for load-bearing structures because of its advantageous mechanical characteristics. Comparable to several wood species of similar density, common reed's hollow, cylindrical stems show remarkable tensile strength (150 MPa) and a modulus of elasticity (8 GPa). The great cellulose concentration in the reed stems is primarily responsible for this strength. The inter-nodal parts show better mechanical performance than the nodal sections, especially among the more than 95% of the stem's length (Albrecht et al., 2023, Köbbing et al.,2013).

Alkali pre-treatment significantly improves the reed's fit as a bio-composite material. Treated reed composites thus show on par with proven wood-based composites bending strengths of roughly 130 MPa and moduli of elasticity ranging from 12 to 13 GPa. This development in bonding quality emphasizes how well alkaline treatment improves the mechanical qualities of bio-composites derived from reeds (Albrecht et al., 2023).

2.3.3 Decomposition and Utilization of reed

Microbial activity characterizes the breakdown of reed cellulose fibers, which accelerates cellulose and hemicellulose degradation relative to lignin, the most resistant component. Nutrient cycling depends critically on this degradation since the breakdown of reed fibers releases carbon, nitrogen, sulfur, and phosphate into the surroundings. Bacterial colonization starts to break down; seasonal fluctuations in fungal activity follow from this and help reed material to break down gradually (Ágoston-Szabó et al., 2006).

Applications for reed in bio-based composites are under increasing research attention. Alkali treatments improve the adhesive characteristics of reed fibers, therefore improving their viability as a sustainable substitute for conventional materials in many different sectors. Understanding the decomposition dynamics and use possibilities of reed fibers, particularly concerning alkali enhancement, emphasizes their dual importance in environmental sustainability and as a helpful source in Bio-composite technology (Ágoston-Szabó et al., 2006).

2.4 Chemical Treatment

2.4.1 Chemical Pretreatments for Natural Fibers

Natural fibers, including flax, hemp, jute, and sisal have drawn much interest due to their environmentally friendly properties and possible use as reinforcement materials in composites. However, their natural properties, including notable moisture absorption and poor fiber-matrix adhesion, require chemical changes to enhance performance (Kabir et al., 2012). This section overviews several chemical pretreatments for natural fibers, with an emphasis on those relevant to reed (Kabir et al., 2012).

2.4.1.1. Hot Water Extraction

Hot water extraction involves submerging fibers in high-temperature water to eliminate water-soluble constituents like hemicelluloses and extractives. In common reed, HWE significantly increased tensile and burst strength, despite a slight decrease in tear strength. It also improved bleachability, enhancing suitability for industrial uses like paper manufacturing (Wang et al., 2013b).

2.4.1.2. Acetylation and Benzoylation

Acetylation and benzoylation are esterification techniques that replace hydroxyl groups with acetyl or benzoyl groups, altering cellulose structure. Acetylation involves the reaction of fiber hydroxyl groups with acetic anhydride, replacing -OH groups with hydrophobic acetyl (–$COCH_3$) groups, which reduce moisture absorption (Kabir et al., 2012).

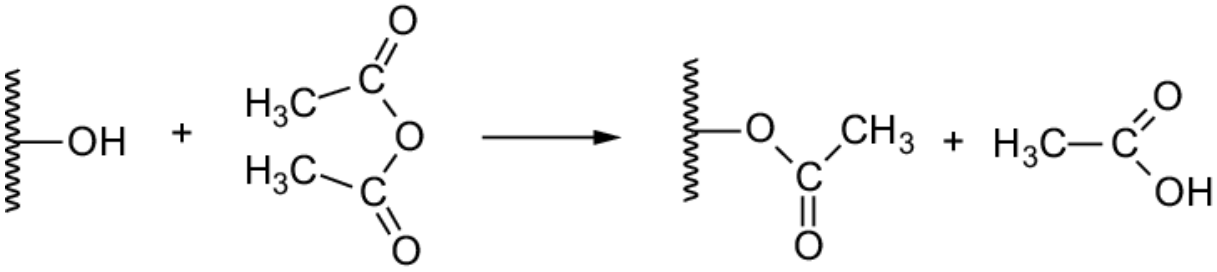

Figure 3 Acetylation Process (Xia et al., 2017)

Equation 1 Acetylation Process (Xia et al., 2017)

$$\boldsymbol{Fibre\text{–}OH + (CH_3CO)_2O \rightarrow Fibre\text{–}OCOCH_3 + CH_3COOH}$$

Benzoylation involves treating fibers with benzoyl chloride, replacing hydroxyl groups with benzoyl groups to improve compatibility with hydrophobic matrices.

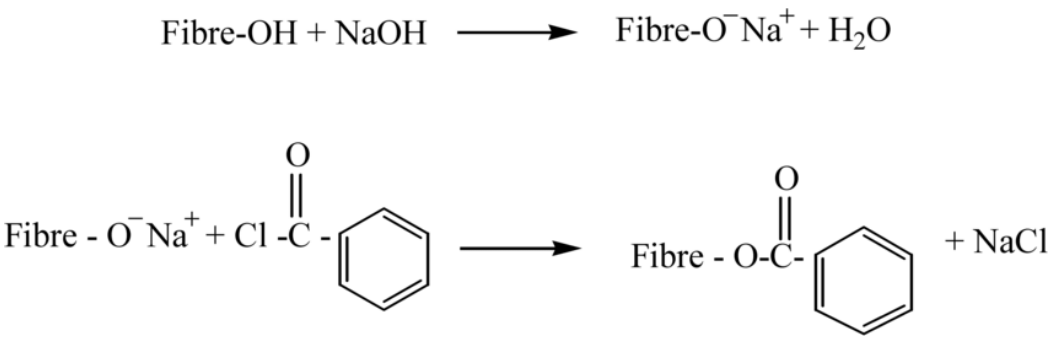

Figure 4 Benzoylation Process (Yadav et al., 2025)

Equation 2 Benzoylation Process (Yadav et al., 2025)

$$\boldsymbol{Fibre\text{–}OH + C_6H_5COCl \rightarrow Fibre\text{–}OCOC_6H_5 + HCl}$$

2.4.1.3. Silane Treatment

Silane coupling agents create chemical links between natural fibers and polymer matrices. In common reed, silane treatment enhances mechanical properties such as tensile strength and flexural modulus by modifying the fiber surface for better matrix compatibility, improving stress transfer and composite efficiency (Kabir et al., 2012).

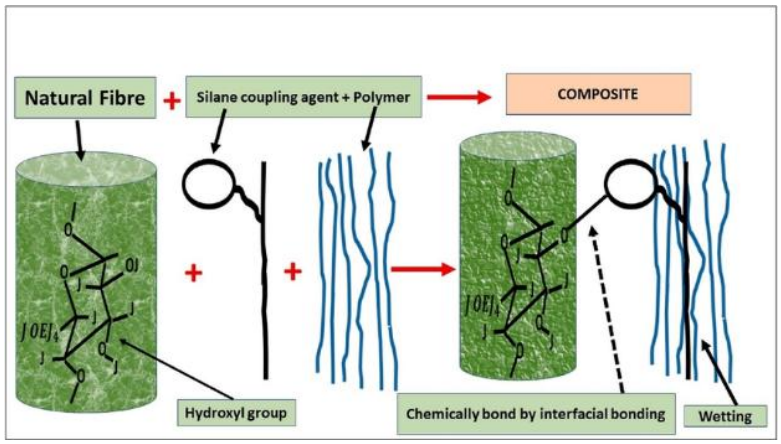

Figure 5 Silane Treatment for natural fibers (Mohanty et al., 2001)

Silane coupling agents hydrolyze and react with hydroxyl groups on fiber surfaces and polymer matrices, forming durable covalent bonds (Xie et al., 2010).

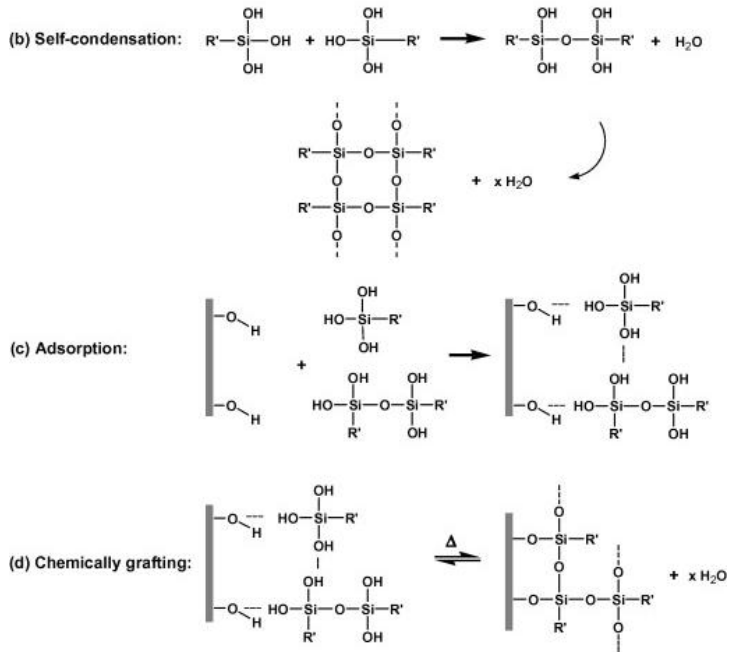

Figure 6 Silane Treatment Equations (Xie et al., 2010)

Table 1 Different treatments for fibers

Treatment Type	**Effect on Fiber Properties**	**More findings**
Hot Water Extraction	Improves strength, reduces tear strength slightly	Increases tensile and burst strength
Acetylation	Reduces hydrophilicity, improves dimensional stability	Increases thermal stability, reduces moisture absorption
Benzoylation	Enhances interfacial bonding	Improves mechanical properties in composites
Silane Treatment	Enhances fiber-matrix adhesion	Increases tensile strength and flexural modulus
Bio sorption	Adsorbs cationic dyes (ex: methylene blue)	Optimal dye removal at pH 8; increased bio sorption with fiber mass

2.4.2 NaOH Pretreatment for Natural Fibers

NaOH, or alkali treatment, is widely used to improve the qualities of natural fibers in textiles, Bio-composites, and biofuels. Immersing fibers in NaOH alters their structure and improves accessibility to enzymes for processes like bioethanol production. NaOH breaks down hemicellulose, lignin, and pectin, exposing more cellulose and enhancing chemical processes.

It also improves dye uptake, tensile strength, fiber flexibility, and fiber-matrix bonding(Uzatici et al., 2022).

Equation 3 NaOH treatment (Williams et al., 2011)

$$\boldsymbol{Fibre\text{–}OH + NaOH \rightarrow Fibre\text{–}O^{-}Na^{+} + H_2O}$$

Table 2 Different fiber characteristics after Alkali treatment

Fibers and Characteristics	**Chemical Composition Changes**	**Crystallinity Changes**	**Thermal Stability**	**Microstructure Changes**
Kenaf Fiber (Ren et al., 2019)	Small increase in density, reduction in diameter	Crystallinity index increases with treatment	Moderate increase in thermal stability	Fiber matrix adhesion improves with treatment
Himalayacalamus falconeri (Pokhriyal et al., 2024)	Cellulose content increases by 6%, density by 4%	Crystallinity index improves from 58.92% to 67.89%	Thermal stability improves from 250°C to 258°C	Better fibrillation and improved mechanical bonding
Raffia Fiber (Elenga et al., 2013)	Increases yellowness and reduces lignin concentration	Initial crystallinity index improvement, but excessive NaOH weakens fibers	Enhanced thermal stability with 5% NaOH treatment	More porous and fibrous structure observed
Lyocell Fabric (Goswami et al., 2009)	Improved dyeability due to structural changes	Conversion to Cellulose II with increased alkali concentration	Higher resistance to moisture absorption	Microstructure becomes more compact with treatment
Hemp Fibers (Sgriccia et al., 2008)	Removes surface impurities, increases fiber density by 2%	Tensile strength and Youngs modulus increase by up to 28%	Thermal stability improves after NaOH treatment	Enhanced fiber-matrix bonding observed under SEM
Jute Fibers (Ray et al., 2001)	Removes non-cellulosic materials, increases crystallinity	12-79% increase in modulus, with treatment beyond 4 hours improving crystallinity	Enhanced heat resistance with alkali treatment	Improved fiber dispersion and adhesion to matrix

2.4.3 Chemical Structure of plant fiber before and after the treatment

NaOH treatment disrupts hydrogen bonding and cleaves ester and ether linkages, removing lignin and hemicellulose. This exposes pure cellulose, increases roughness and porosity, and improves reactivity. It enhances mechanical interlocking and bonding in composites, increases tensile strength and stiffness, and reduces moisture absorption (Uzatici et al., 2022).

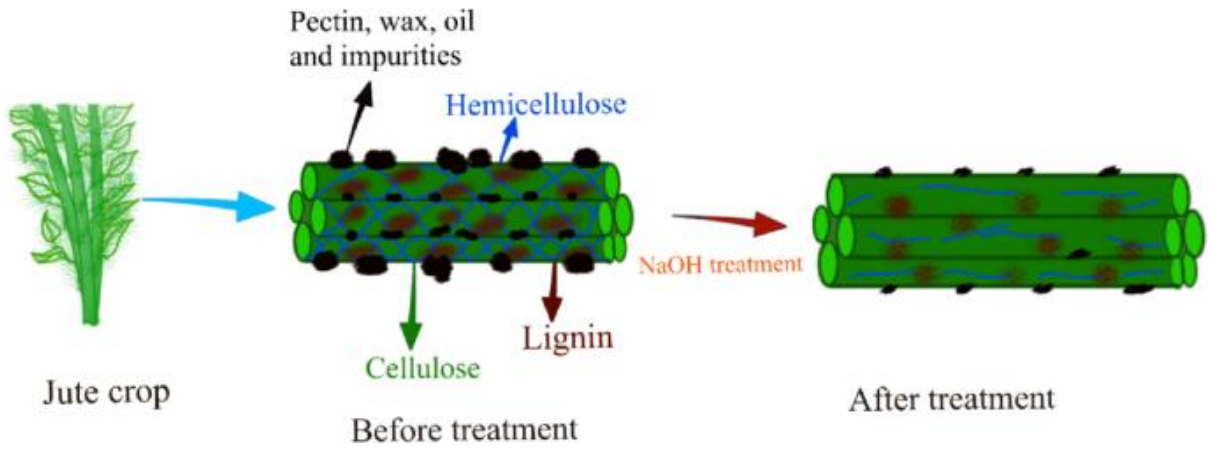

Figure 7 Jute fibers before and after treatment (Kaysar et al., 2024)

2.5 Polymers and bio-composites

Bio-composites based on polylactic acid (PLA) have attracted increasing attention due to PLA's biodegradability, renewability, and acceptable mechanical properties. PLA composites reinforced with natural fibers, such as jute or flax, benefit significantly in tensile strength and stiffness, especially when post-tensioning techniques are used (Hinchcliffe et al., 2016). Pre stressed PLA composites enhanced tensile specific strength by 116% and stiffness by 62% over unreinforced PLA, primarily due to optimized fiber alignment and strong interfacial bonding (Hinchcliffe et al., 2016). PLA composites can be tailored for both disposable and durable applications by incorporating fibers, nano fillers, and additives to compensate for its inherent brittleness and low thermal resistance (Murariu et al., 2016)

High-density polyethylene (HDPE) composites present a different profile, offering excellent toughness and chemical resistance, though the hydrophobic nature of HDPE poses interfacial challenges with natural fibers (Zhang et al., 2011). Adding alumina fillers significantly enhanced both thermal conductivity and tensile strength of HDPE composites, with smaller particles (e.g., 0.5 µm) yielding superior performance due to improved dispersion and interfacial area (Zhang et al., 2011).

Polypropylene (PP) is widely used in bio-composite applications due to its favorable cost, mechanical properties, and processability. Nevertheless, like HDPE, it suffers from poor compatibility with hydrophilic natural fibers. A 50 wt% kenaf-filled PP composite, compatibilized with maleated PP, achieved tensile and flexural moduli comparable to or exceeding conventional PP-mica or glass-filled systems, while offering the added advantages of low density and renewability (Sanadi et al., 1994). Similarly, the fabrication of unidirectional all-PP composites using highly oriented PP tapes, achieving high tensile moduli (up to 13 GPa) with minimal thermal degradation through controlled hot compaction techniques (Alcock et al., 2005).

2.6 Processing Methods for bio-composites

The processing method has profound implications for the functioning of a bio-composite. Manufacturing techniques influence properties such as strength, longevities, and even how easily material may be deformed or shaped. Keeping the right proportion and flow during processing is essential to a thermoplastic bio-composite made of composites with a plastic matrix and fillers derived from biological sources. Principal processing techniques widely used in research and development, Micro-compounding, extrusion, injection molding, and melt flow index testing are discussed in this section.

2.6.1 Twin-Screw Micro-compounding

Micro-compounding allows to work with small amounts of materials usually no more than a few grams. It is especially valuable when testing new or expensive polymers and additives. On a much smaller scale, twin-screw Micro-compounders like the DSM Xplore system are configured to mimic the high-shear mixing component of commercial extrusion. These machines are best suited for first-stage material development since they offer better control of processing temperature, screw speed, and mixing force. Several studies have demonstrated how effectively Micro-compounding dispenses additives in a polymer matrix. This process radically altered mechanical and barrier properties when PP was compounded with modified clays. Material degradation is reduced by low residence time and rigorous parameter control, a common problem when handling temperature-sensitive polymers (DSM Xplore, 2016).

2.6.2 Extrusion

In industry and research, extrusion is a standard method for generating continuous lengths of composite material. Pushing the polymer through a die, it is melted and combined with additives. Ideal for manufacturing composite pellets or films that can subsequently be molded or shaped, the method is very scalable.

Modern lab-scale extruders, like the Thermo Scientific Process 11, are quite adaptable for testing various material configurations since they have modular screw designs and several heating zones. The design provides exact control over temperature, pressure, and mixing intensity. Improper mixing or overheating can cause fiber breakage, bad dispersion, or matrix degradation. Thus, this degree of control is crucial. Often, extrusion is used to prepare granules from compounded materials. Molding techniques using these granules generate test samples. Studies show regularly that the mechanical characteristics and uniformity of the final product are directly affected by the quality of mixing during extrusion (Thermo Fisher Scientific Inc., 2019).

2.6.3 Injection Molding

Injection molding usually forms the compounded, granulated material into test samples. This technique injects the material into a mold under high pressure after heating it until it flows. It is a quick and effective technique that is particularly beneficial for producing consistent mechanical or thermal testing samples. Built for accuracy and repeatability, lab-scale injection molders such as the Xplore IM12. All of these factors influence the final shape and quality of the specimen; therefore, they let the operator regulate the mold temperature, injection pressure, and holding time. These systems are designed to work flawlessly with microcomputers, ideally suited for research laboratories (Xplore Instruments BV, 2021).

Especially for thermoplastic composites, injection molding is quite beneficial since it helps to align fillers and remove air voids. However, because of their sensitivity to heat and moisture, some plastics, such as PLA, need close handling during this process. The approach is necessary to convert lab-scale formulations into physical samples that can be evaluated for strength, flexibility, and durability.

2.6.4 Melt flow index

The Melt Flow Index (MFI) is a widely used tool to understand how thermoplastic materials behave when they're melted. Essentially, it tells us how easily a plastic flows when heated and pushed through a small opening. This is really useful for manufacturers during quality checks, product development, and when comparing different types of plastics. Getting accurate and reliable MFI results depends a lot on how the equipment is set up and maintained. To keep things running smoothly, operators use specific tools, to clean the chamber, compacting tools to load the material properly, and split-head tools to help with safe and thorough cleaning. It's also important to avoid using strong solvents on the outside of the machine, as these can damage the paint or sensitive screens.

The machine's built-in cutting device also plays a big role in test accuracy. If the blades aren't aligned or adjusted properly, the plastic pieces might not be cut evenly. To prevent that, operators should make sure the blade tip stays at least 1 mm away from the center of the die's rotation, and reassemble everything carefully to avoid clashes with internal parts. MFI test is a standardized method used to evaluate the flow characteristics of thermoplastics under specific conditions of temperature and load. This property is commonly expressed as either the Melt Flow Rate or the Melt Volume-Flow Rate, as described in international standards such as ISO 1133 and ASTM D1238 (ISO 1133: Melt Flow Index (MFI) Plastics).

The MFI test measures the ease of flow of a thermoplastic polymer through a standardized die under specified temperature and pressure conditions.

The MFI is calculated using the formula:

Equation 4 Melt flow index (YASUDA SEIKI SEISAKUSHO, LTD., 2025)

$$MFI(T, M_{nom}) = \frac{600 \times m}{t}$$

Where:

- T is the test temperature (°C)
- M_{nom} is the nominal applied load (kg)
- m is the mass of the extrudate (g)
- t is the time interval (s)

2.7 Characterization of bio-composites

2.7.1 Fourier-Transform Infrared Spectroscopy Analysis

FTIR is a technique that is usually harnessed to study the chemical behavior of natural fibers, either by alkalis treatment, such as sodium hydroxide, or both. The principle of the technique is that it allows one to measure the absorption of infrared light by molecules as a consequence of specific vibrations that molecular chemical groups undergo in correspondence with their chemical structure. With plant-based fibers, applying FTIR may help show modifications in primary constituents such as cellulose, hemicellulose, and lignin.

One essential aspect in which FTIR is useful is its capability to detect specific functional groups such as hydroxyl, carbonyl, and ether, or even cross-links related to fiber composition and structure. These functional groups may shift, weaken, or even disappear due to the influences of sodium hydroxide on fibers. In all such situations, FTIR will detect these changes. Therefore, it is possible to correlate how, within the molecular level, the chemical bonds responsible for the internal structure of the fiber have changed (Kavkler et al., 2011).

FTIR is mainly used to assess crystallinity changes after assessing the treatment, essentially in terms of how ordered or disordered the cellulose structure has turned out following treatment. Some peaks' infrared spectra for example, their intensity comparisons are valid when tracking the structural transformation of fiber (Carrillo et al., 2004).

2.7.2 Optical Microscopy

Optical microscopy is a simple approach to visually check the surface of natural fibers before and after treatment when trying to grasp the physical results of alkaline treatment, such as how the surface texture changes or whether the fibers exhibit damage, swelling, or splitting. Important for composite applications is the fibers' ability to bond with other materials; thus, the apparent changes have a significant impact.

This method also helps one compare fibers treated under various conditions. It can highlight variations in how the treatment affects fiber structure, guiding choices on which condition causes the most desired changes. Some research even uses microscopy to investigate how the

fibers interact with polymers in bio-composite materials, displaying how well they blend and adhere to one another (Ouajai & Shanks, 2009).

3 Methodology

This section presents the methodology used for the surface treatment of reed fibers and the preparation of bio-composites composed of 20% reed fiber and 80% polymer using PP, PLA, and HDPE as matrix materials. The procedures for processing untreated and treated fiber composites are explained in detail. Furthermore, this section describes the analytical techniques applied, including FT-IR spectroscopy for identifying chemical modifications and optical microscopy for examining the microstructure of granules from the six different composite formulations, including both treated and untreated fiber composites.

3.1 Chemical Treatment for Reed fibers

3.1.1 Alkali Treatment using NaOH

This study utilized common reed as a raw material for fiber treatment. Reed classified as a lignocellulosic plant, meaning they contain significant amounts of cellulose, hemicellulose, and lignin within their cell walls. A fiber treatment protocol originally developed for hemp at the University of Borås, Sweden, was adapted for use with reed and some minor adjustments were made for differences in fiber thickness and surface texture (Skrifvars & Arya, 2023).

3.1.1.1. Grinding

The reed stalks were first dried and then mechanically ground using a RETSCH SM 100 cutting mill. The grinding process reduced the material into smaller fragments suitable for sieving and chemical treatment. The grinding was carried out in small increments, and the system was periodically cleared to maintain operational efficiency.

3.1.1.2. Sieving

Once ground, the reed biomass was sorted by size using a sieve shaker equipped with mesh openings of 2 mm, 1 mm, and 0.5 mm. Only the fraction that passed through the 2 mm sieve and was retained by the 1 mm sieve was selected for further processing. This particle size range was chosen to ensure uniformity, which is important for consistent fiber dispersion in composite matrices and for minimizing stress concentrations in the final material.

3.1.1.3. Washing

The collected samples were washed to remove dust and other fine residues generated during grinding. The material was placed in the smallest sieve (0.5 mm) and rinsed with clean water until the outflow appeared clear. This is to ensure surface impurities were eliminated, reducing the risk of interference during chemical treatment and improving overall fiber quality.

3.1.1.4. Alkali treatment (NaOH Soaking)

The cleaned and sieved fibers of 500-600g were soaked in a 4.5% (w/w) sodium hydroxide (NaOH) solution for a duration of five hours at room temperature (Skrifvars & Arya, 2023).

After soaking, the fibers were rinsed several times with distilled water until a neutral pH was reached. Once neutralized, the treated fibers were oven-dried at 80°C for 24 hours to remove residual moisture. This drying process preserved the fiber structure and ensured readiness for subsequent processing stages such as compounding or thermal molding (Ouajai & Shanks, 2009).

Figure 8 NaOH treatment at the laboratory

3.2 Processing Methods

This section outlines the processing steps used to produce the reed composites from three polymers as mentioned earlier each reinforced with 20 wt% treated or untreated reed biomass. The process can be defined with two stages: Micro-compounding and injection molding. Micro-compounding is used to uniformly blend reed fibers with polymer matrices at a small scale, while injection molding is to shape these compounded blends into standardized test specimens for further analysis. The polymer-fiber blends were processed separately under optimized conditions based on each polymer's thermal and rheological properties.

3.2.1 Micro-compounding

Micro-compounding was performed using a DSM Xplore 5 Micro-compounder equipped with rotating twin screws. Each polymer 80%(80g of mass) was compounded with 20% (20g of mass) fiber content in separate batches. The polymer pellets were first dry-blended with the fibers and then introduced into the compounder manually. A nitrogen atmosphere was used during processing to minimize thermal degradation, particularly important for more sensitive polymers such as PLA.

Table 3 Parameters for Micro-compounding

Polymer Type	Temperature Range (°C)	Screw Speed (rpm)	Residence Time (min)
PLA	170–190	100	3–5
PP	180–200	100	3–5
HDPE	170–190	100	3–5

These temperatures were selected to ensure complete melting of the polymer without causing thermal degradation. Screw speed was maintained at 100 rpm for all materials to balance shear mixing and minimize fiber breakage. Each batch was recirculated for 3 to 5 minutes, allowing sufficient time for the fibers to disperse uniformly throughout the molten polymer. The compounded blends were extruded as continuous strands, air-cooled, and pelletized. The pellets were then sealed and stored under dry conditions until further use.

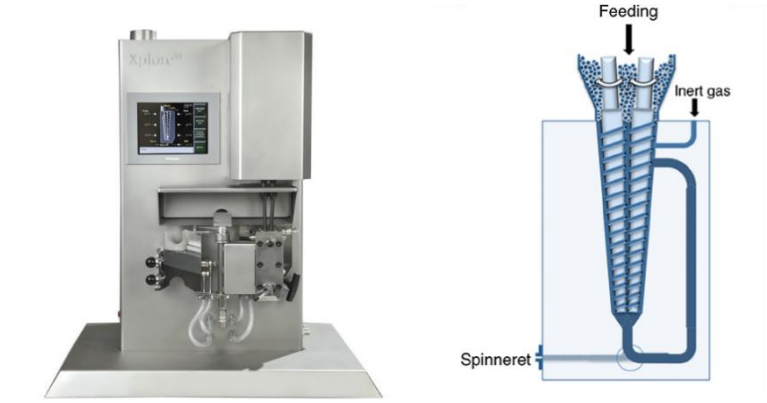

Figure 9 Twin screw micro-compounder (Hooshmand et al., 2014)

3.2.2 Injection molding

Injection molding was performed using the IM-12 benchtop injection molding machine, fitted with a single-cavity aluminum mold designed to produce specimens by ASTM D638 Type I dimensions.

Before starting the molding, the prepared composite pellets were loaded into the machine's hopper. The injection pressure was kept between 100 and 120 bar to fill the mold. After injection, a short holding pressure was applied for 5 to 10 seconds to help pack the material and reduce internal voids. The mold was maintained between room temperature and 50 °C to allow the samples to cool and solidify efficiently.

Each molding cycle took around 20 to 30 seconds from start to finish. The mold was opened once the material had cooled, and the finished dog bone-shaped specimens were carefully removed by hand. Each sample was checked for common molding issues like short shots, warping, or excess flash. Only specimens that passed visual inspection were kept. These were then stored in desiccators to protect them from moisture until testing.

Figure 10 Injection Molder (Xplore Instruments, 2019)

Table 4 Parameteres for Injection molder

Machine	IM-12 Injection Molding Machine
Specimen geometry	ASTM D638 Type I (dog bone)
Injection temperature	PLA: 180–190 °C PP: 200–210 °C HDPE: 180–190 °C
Mold temperature	Ambient to 50 °C
Injection pressure	100–120 bar
Holding pressure	60–80 bar
Holding time	5–10 seconds
Cycle time	20–30 seconds

3.3 Melt Flow Index

The MFI test was performed using mass-based in accordance with ISO 1133:2005 standards. Before starting the test, the appropriate temperature and load were selected based on the polymer's technical datasheet, ensuring the conditions matched the material's flow behavior. The machine was set to the specified temperature, and a sample weighing between 4 to 8 grams was carefully measured and gently poured into the preheated barrel to avoid introducing air pockets (Plastics — Determination of the Melt Mass-flow Rate MFR) and the Melt Volume-flow Rate (MVR) of Thermoplastics, 2005). The grade used in this work, Braskem C705-44NA HP, is an injection-molded impact copolymer. It is easy to process, shows a melt flow rate of 44 g/10 min, and has good mechanical properties, including a tensile strength of roughly 28 MPa and significant impact resistance. Its thermal stability lets it withstand processing temperatures of up to 260°C (Data Sheet C705-44NA HP, 2019). PLA grade used in this study is Ingeo™ 4043D. It is widely recognized for its excellent clarity, stiffness, and environmental sustainability. Ingeo 4043D has a tensile strength of 60 MPa at yield and a tensile modulus of 3600 MPa, with 22 a melt flow rate of 6.0 g/10 min at 210°C (2.16 kg). This work examines the HDPE (DOW 25055E) with a melt flow index of 25 g/10 min, a tensile strength of roughly 25 MPa, and an elongation at a break of about 200%. Its high softening point (about 124°C) and good processing qualities make it an excellent material for injection molding since it keeps its shape even under heat (Polypropylene, UNIPOL Technology, Dow, Applications, Properties, Plastic, Polymer, Thermoplastic).

Figure 11 Melt flow index machine (A-MELT)

Table 5 Parameters for MFI (ISO 1133: Melt Flow Index (MFI) Plastics, 2005)

Polymer	**Melt flow rate (g/10 min)**	**Temperature and load**	**Test Method**
Polylactic Acid 4043 D	6.0 g/10min	210 ℃ / 2.16 kg	ASTM D1238
High density polyethelene HDPE 25055E	25.0 g/10min	190 ℃ / 2.16 kg	ISO 1133
PP C705-44NA HP	44 g/10 min	230 ℃ / 2.16 kg	ISO 1133

Once the sample was loaded, the piston was inserted, and a timer was immediately started for 300 seconds to allow the material to fully melt and stabilize at the set temperature. After this heating period, the designated test load was applied, and the cut timer was simultaneously activated. The duration of the cut timer was based on the expected MFI value of the polymer, with higher flow materials requiring shorter intervals (Plastics — Determination of the Melt Mass-flow Rate (MFR) and the Melt Volume-flow Rate (MVR) of Thermoplastics, 2005).

Table 6 Experimental Parameters (ISO 1133: Melt Flow Index (MFI) Plastics, 2005)

MFR (g /10 min)	Mass of test sample in cylinder (g)	Extrudate cut-off time interval (s)
≥ 0.1 but ≤ 0.5	3 to 5	240
> 0.5 but ≤ 1	4 to 6	120
> 1 but ≤ 3.5	4 to 6	60
> 3.5 but ≤ 10	4 to 8	30
> 10	4 to 8	5 to 15

As the molten polymer began to extrude through the die, it was manually cut and collected at each cut interval until the marker in the piston reached the upper edge of the cylinder. These collected samples were later weighed to calculate the melt flow rate. Following the test, the equipment was cleaned while still warm using non-abrasive tools such as a soft cloth to ensure no residue remained and to preserve the condition of the barrel, die, and piston for future testing.

3.4 FT-IR Analysis

Fourier Transform Infrared (FTIR) spectroscopy was initiated to analyze alkali-treated and untreated biomass samples and investigate chemical modifications induced by the treatment. The analysis used the Thermo Scientific™ Nicolet™ iS™5 FT-IR spectrometer equipped with a Thermo Scientific™ iD7 Attenuated Total Reflectance (ATR) accessory. The iD7 ATR

features a monolithic diamond crystal with all-reflective optics, offering robust spectral performance across a broad infrared range and high throughput (Thermo Fisher Scientific Inc., 2021).

Multiple sample types were prepared to accommodate variations in fiber morphology. These included:

- Large-sized fibers
- Small piles of loose and fine fibers

The samples were manually pressed onto the diamond ATR crystal using the accessory's integrated pressure tower to ensure good contact, essential for optimal spectral quality in ATR-FTIR measurements. For each sample, spectra were recorded across the mid-infrared range. Particular attention was given to ensuring consistent sample contact and pressure application across different sample sizes. The obtained spectra were subsequently analyzed using Thermo Scientific™ OMNIC™ software, allowing baseline correction, peak identification, and comparison between treated and untreated samples.

Figure 12 FTIR technique and spectrometer (Thermo Fisher Scientific Inc., 2021)

3.5 Optical Microscopy experiments

An optical microscopy experiment examined the surface morphology and structural integrity of untreated and alkali-treated reed fibers-polymer composites. All imaging was performed using a Zeiss Axio Imager A1 upright optical microscope (Carl Zeiss MicroImaging GmbH, 2008).

Pre-prepared composite samples were used for this investigation. Thin sections of each sample were mounted on standard glass slides without additional staining or chemical treatment. Observations were conducted using magnifications of 5×, 10×, and 20× to capture overall structure and finer surface details. Both RL and TL imaging modes were utilized to reveal different aspects of the samples. To enhance contrast and surface clarity, a dark filter was applied during imaging, particularly under reflected light. Images were acquired to preserve image quality for subsequent analysis.

The field and condenser diaphragms were adjusted accordingly, and both bright field and dark field modes were applied based on the sample's visual characteristics.

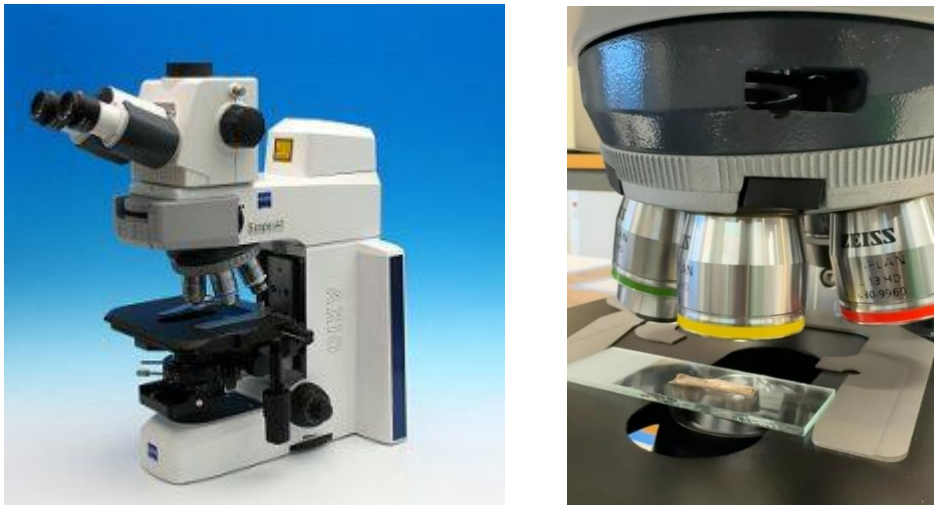

Figure 13 Optical Microscope (Axio Scope.A1 - LABORSCIENCE A.E., 2017

4 Results

4.1 Optical Microscopy Image Analysis

High-resolution images were obtained from thin-sectioned specimens of the composite materials developed during this study (PP, PLA and HDPE with Alkali treated and untreated reed). Additionally, microscopy imaging was conducted on reed fiber derivatives including cellulose, holocellulose, and lignin that had been extracted through previous experimental procedures.

Table 7 Microscopy Images and specifications

Microscopy Image of the sample	Comments on sample
	Lignin 10x magnification under reflected light and the dark filter
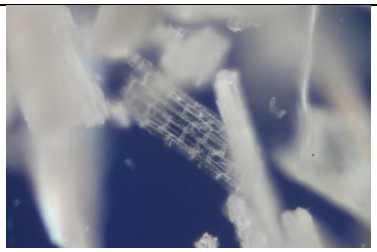	Holocellulose 20x magnification under transmitted light and the bright filter
	Cellulose 5x magnification under transmitted light and bright filter

These fiber components were extracted in a previous experiment done for the fiber analysis, and these have been dried under 105℃ for 24 hours.

Table 8 PP + reed fiber composite microscopy images

PP + Common reed Fiber	
Untreated Fiber with Polymer	**Treated Fiber with Polymer**
 A Magnification: 10x Imaging mode: RL/DF	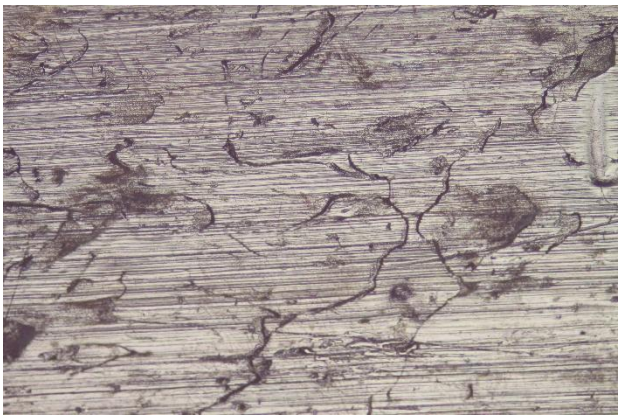 C Magnification: 5x Imaging mode: RL/BF
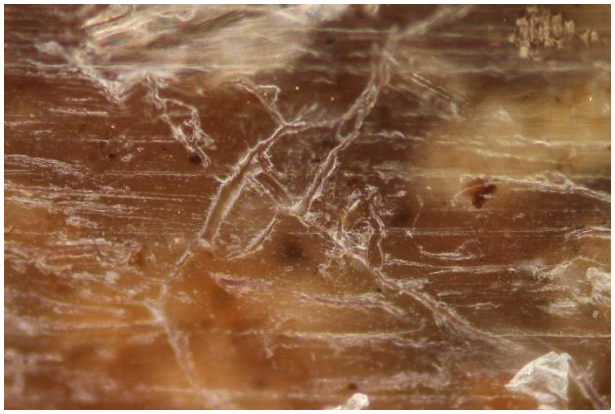 B Magnification: 5x Imaging mode: RL/DF	 D Magnification: 20x Imaging mode: RL/DF

For PP + Common Reed Fiber**,** the untreated fiber A shows a jagged, rough surface with visible strands and a brown color tone. Treated fiber surfaces B appear more even, with visible cracks or line patterns and a uniform light coloration. One treated image D reveals a granular texture with small fragments and noticeable pit-like voids, while another shows shiny, webbed line features. Overall, the treated samples display finer and more detailed surface characteristics

Table 9 HDPE reed fiber composite microscopy images

HDPE + Reed Fiber	
Untreated Fiber with Polymer	**Treated Fiber with Polymer**
 A Magnification: 5x Imaging mode: TL/BF	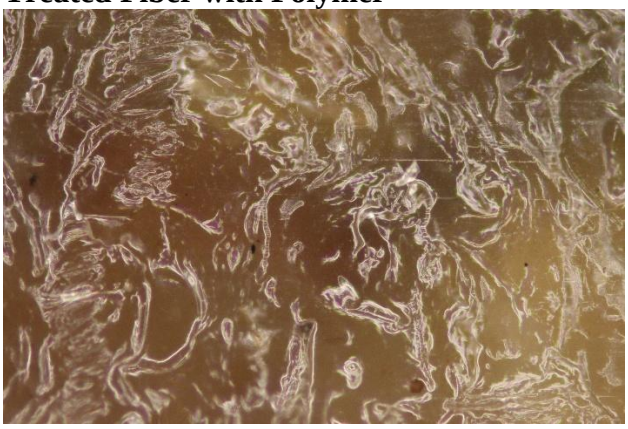 C Magnification: 10x Imaging mode: RL/BF
 B Magnification: 5x Imaging mode: RL/DF	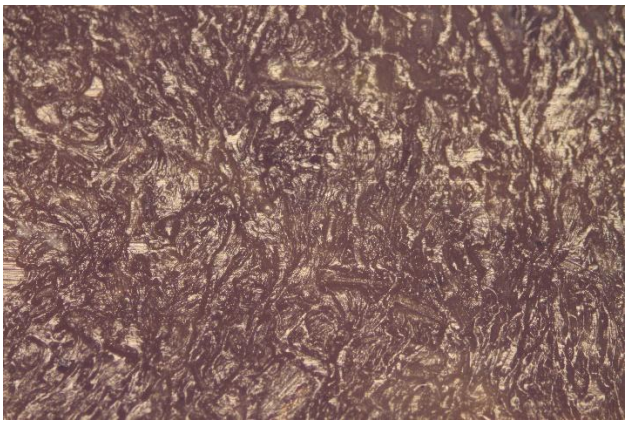 D Magnification: 10x Imaging mode: Rl/BF

In the HDPE + Reed Fiber composites, the untreated fiber A image reveals large, dark fragments contrasting sharply against a light background, suggesting a scattered material appearance. Treated samples C, D exhibit wavy, semi-transparent structures with a glossy, brown tone. The lower images show a dense, speckled texture with no sharp voids and an overall darker, more uniform surface appearance, with fine, evenly spread light streaks.

Table 10 PLA + reed fiber composite microscopy images

<table>
<tr><th colspan="2">PLA+ Reed Fiber</th></tr>
<tr><td>Untreated Fiber with Polymer
 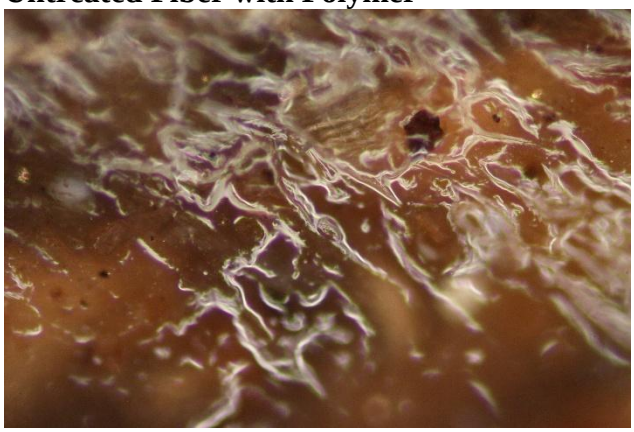
A
Magnification: 20x
Imaging mode: RL/DF</td><td>Treated Fiber with Polymer
 
C
Magnification: 5x
Imaging mode: RL/DF</td></tr>
<tr><td> 
B
Magnification: 5x
Imaging mode: RL/DF</td><td> 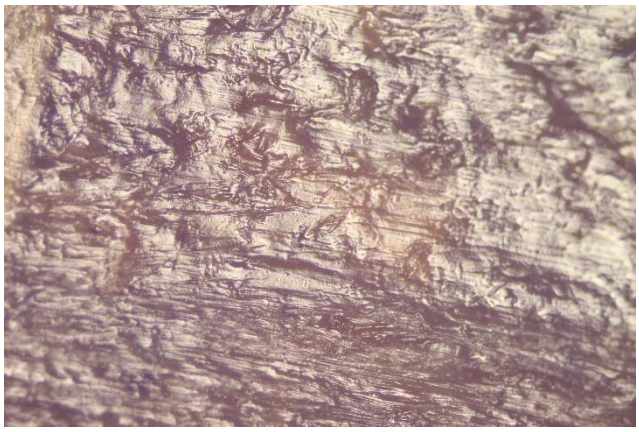
D
Magnification: 10x
Imaging mode: RL/BF</td></tr>
</table>

The microscopy images of PLA+ Reed Fiber composites show noticeable surface differences between untreated and treated fibers. The untreated fiber A displays a rough texture with uneven material distribution and bright reflective regions. In contrast, treated fiber surfaces C and D appear smoother and more uniform, with aligned fibrous patterns and lighter, more consistent tones. These treated surfaces show fewer irregularities and a more compact texture in comparison to the untreated ones.

4.2 FTIR Analysis and Interpretations

4.2.1 FTIR of Untreated Reed Fiber Samples

The FTIR spectra of seven untreated reed biomass samples reveal a typical lignocellulosic profile, and the peaks confirm the presence of intact lignocellulosic architecture and it can be summarized like below table; (Linderbäck et al.,2024)

Table 11 FTIR for untreated fiber samples

Wavenumber (cm^{-1})	**Bond / Functional Group**	**Explanation**
3600–3100	O–H stretching	Broad band due to hydroxyl groups in cellulose and hemicellulose; affected by hydrogen bonding and moisture content.
2917–2850	C–H stretching	From aliphatic $–CH_2$ groups present in cellulose and hemicellulose.
1730–1733	C=O stretching	From acetyl and ester groups in hemicellulose and lignin.
1634–1600	O–H bending / Aromatic C=C	O–H bending of absorbed water or skeletal vibrations of lignin's aromatic rings.
1510–1450	Aromatic C=C / C–H bending	Vibrations from aromatic rings and C–H deformation in lignin.
1240–1252	C–O–C asymmetric stretching	Typical of ether bonds linking hemicellulose and lignin.
1030–1050	C–O and C–C stretching	Strong band from cellulose and hemicellulose backbone structures.
898	β-glycosidic linkage	Characteristic of crystalline cellulose structure.

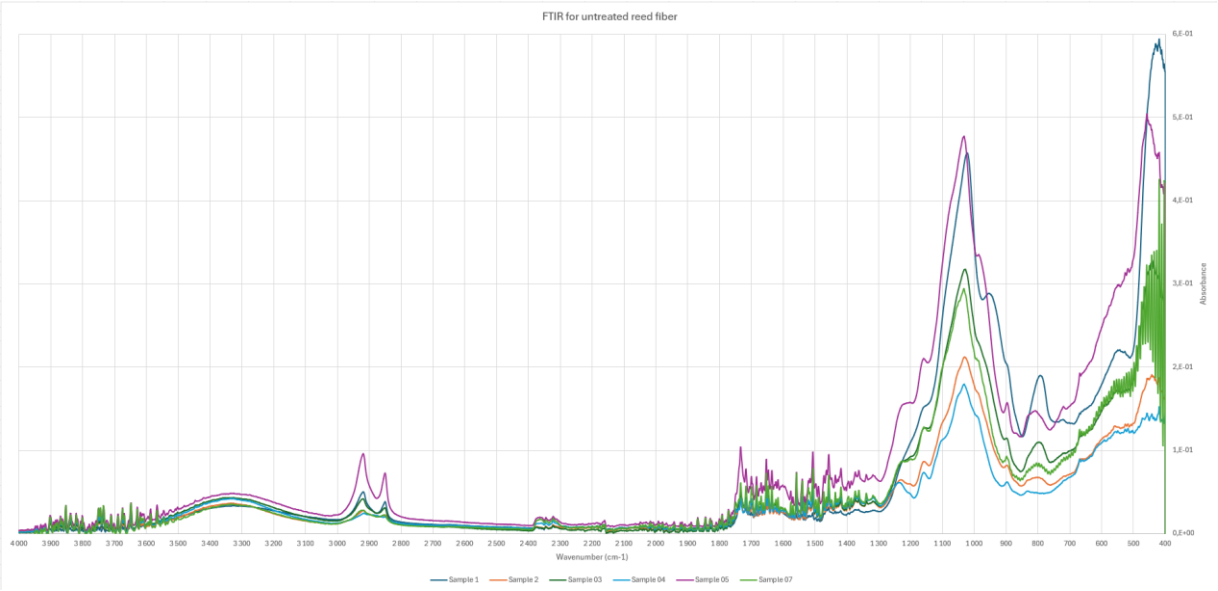

Figure 14 FTIR graph for untreated fibers

4.2.2 FTIR of NaOH treated Reed Fiber Samples

7 samples of NaOH treated biomass, main spectral shifts indicate structural purification, and the wavenumbers with the bonding are summarized below table;(Jayamani et al., 2020; Uzatici et al., 2022)

Table 12 FTIR for Alkali treated reed fibers

Wavenumber (cm^{-1})	**Observed Change After NaOH Treatment**
3600–3100	O–H band becomes sharper and stronger
1730	C=O band disappears
1600–1450	Reduced intensity of aromatic ring and C–H bending vibrations
1240–1250	Lower intensity of C–O–C asymmetric stretching
1030 and 898	Sharpened and persistent peaks

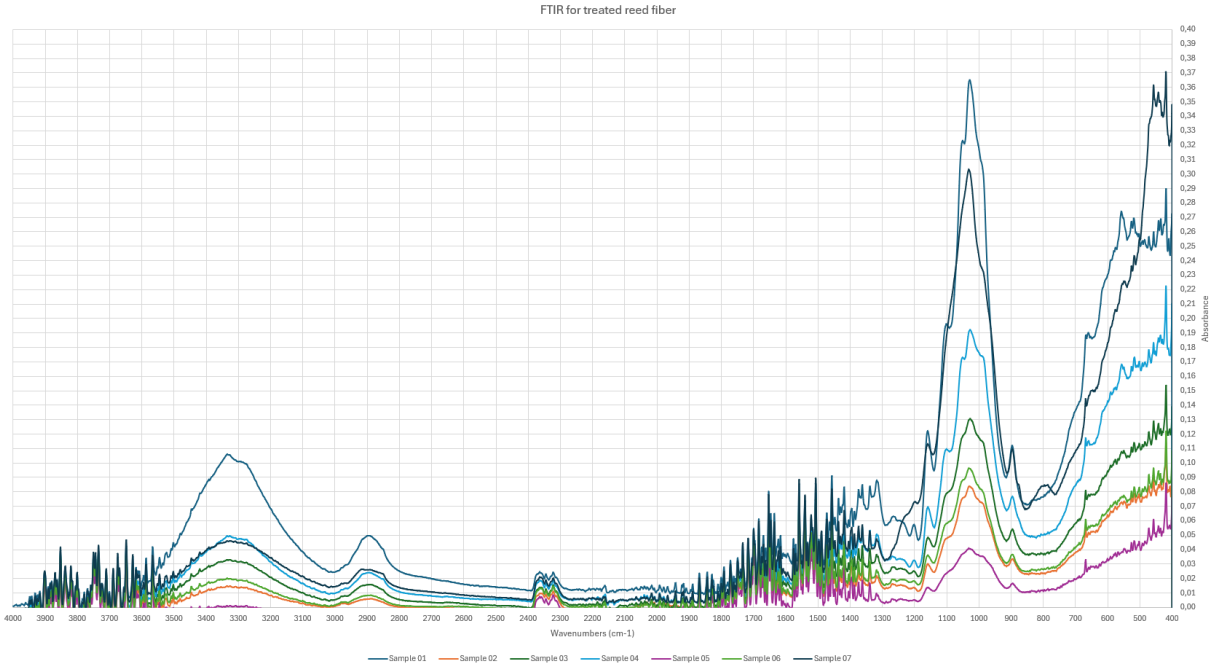

Figure 15 FTIR for Alkali treated reed fibers

4.2.3 FTIR comparison for treated and untreated fibers

After NaOH treatment, the FTIR spectra of reed fibers show clear signs of structural purification. The sharpening of the O–H band (3600–3100 cm^{-1}) indicates the removal of hemicellulose and lignin, exposing more free hydroxyl groups in cellulose. The disappearance of the C=O peak at 1730 cm^{-1} confirms deacetylation of hemicellulose, while reduced intensity in the 1600–1450 cm^{-1} region suggests partial lignin removal. Weakened C–O–C bands (1240–1250 cm^{-1}) reflect cleavage of ether linkages, and the sharpening of peaks at 1030 and 898 cm^{-1} highlights preserved and increasingly crystalline cellulose.

Table 13 Wavenumbers and Interpretations

Region (cm^{-1})	Interpretation of Change After NaOH Treatment
3600–3100	O–H band becomes sharper and more defined; indicates removal of hemicellulose/lignin and exposure of cellulose hydroxyls.
2917–2850	Minor change; aliphatic C–H bonds in cellulose remain mostly unaffected.
1730	Peak disappears; confirms deacetylation and removal of hemicellulose.
1600–1450	Decreased intensity; indicates partial removal of lignin aromatic structures.
1240–1250	Weakened; corresponds to cleavage of ether linkages between lignin and hemicellulose.
1030	Remains strong or sharpens; confirms cellulose preservation and increased purity.

898	Sharpens; indicates increased crystallinity and exposure of β-glycosidic cellulose linkages.

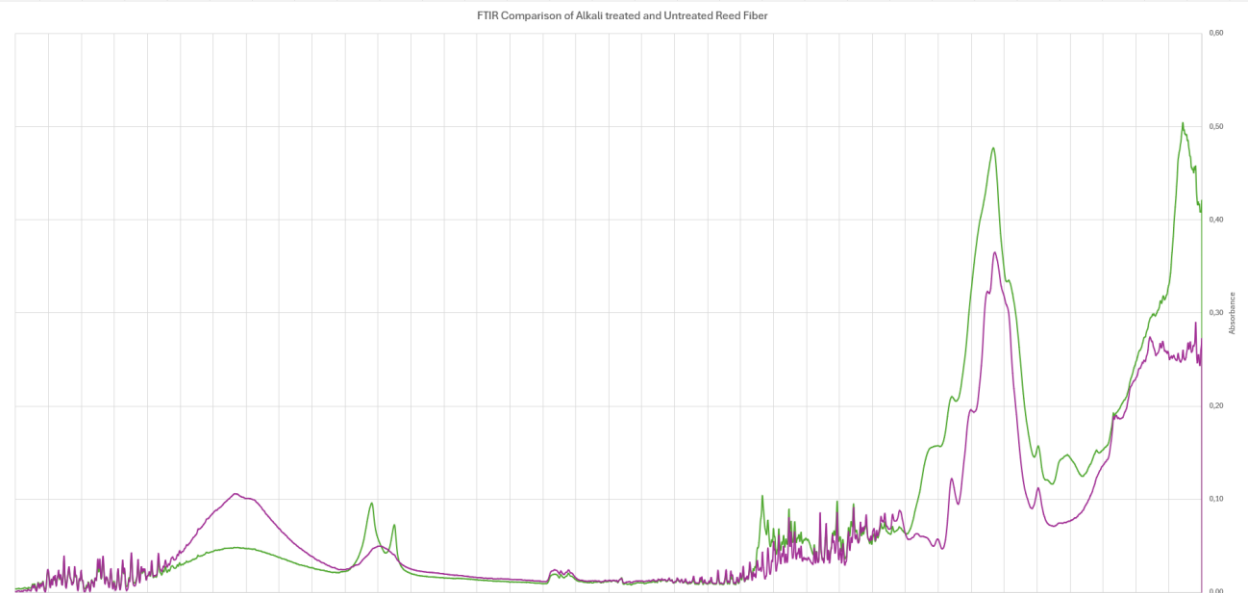

Figure 16 Comparison of treated and untreated fibers

4.2.4 Unusual Peaks and Their Possible Origins

In addition to typical lignocellulosic peaks, the spectra reveal some unusual minor peaks, particularly in the 2400–2300 cm^{-1} range. These are not common in standard plant fiber spectra and may stem from:

- Atmospheric Interference: Peaks in the 2400–2350 cm^{-1} region are often due to ambient CO_2 absorption during measurement (Smith, 2024).
- Silicon-Related Vibrations: Given the high silicon content in Phragmites australis (Brackhage et al., 2013)(accumulated as silica or phytoliths in leaf and stem tissue), these peaks may also correspond to:
    - Si–O asymmetric stretching overtones
    - Combination bands of Si–OH or Si–H (Brackhage et al., 2013)

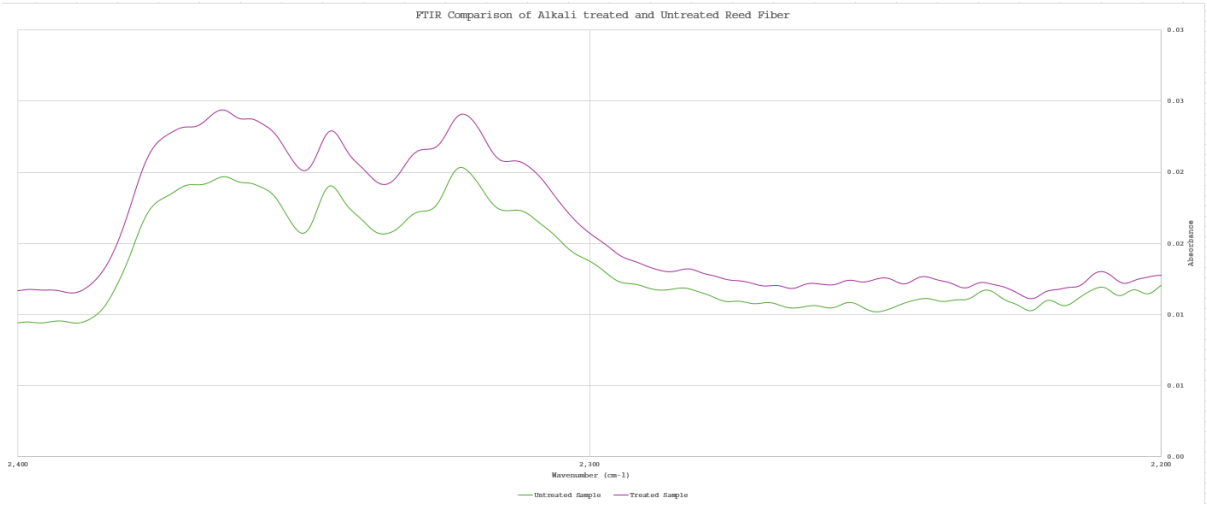

Figure 17 2400 cm^{-1} to 2200 cm^{-1} peak explanation

In the 3000–2800 cm^{-1} region, untreated reed fibers typically exhibit a doublet, corresponding to asymmetric and symmetric C–H stretching vibrations of –CH_2 groups from both cellulose and hemicellulose**.** This dual peak is a result of overlapping signals from multiple components, especially the amorphous fractions.

After NaOH treatment, this region often shows a single, merged peak or a narrower band, which suggests the removal of hemicellulose and surface-bound impurities. With the reduction of chemical diversity, particularly the loss of less ordered structures, the spectral contributions simplify, leaving a dominant signal from the cellulose backbone. This transformation supports the notion of increased chemical homogeneity and higher crystallinity in the treated fibers.

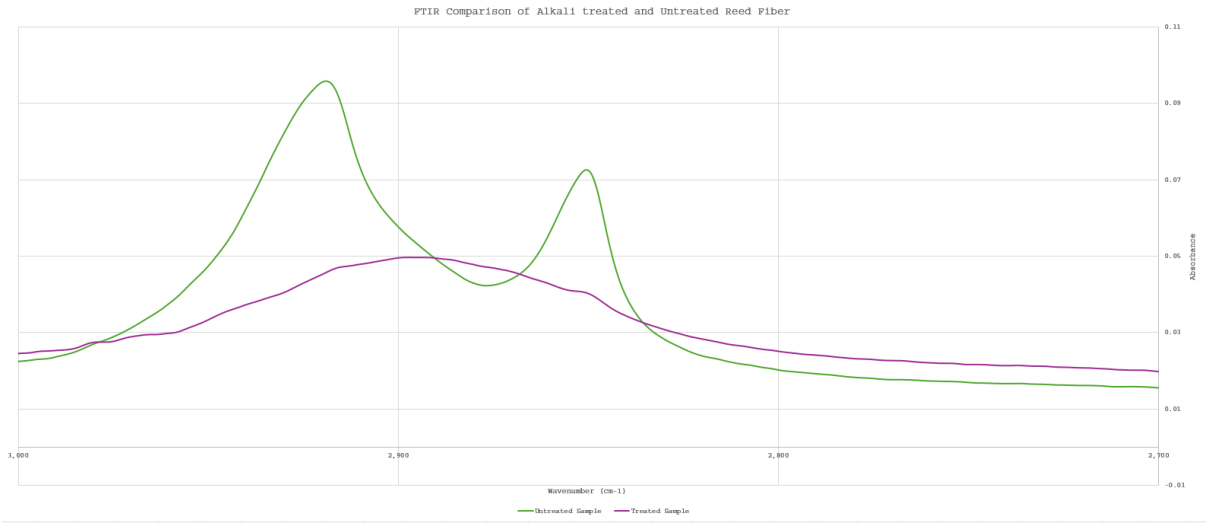

Figure 18 3000 cm^{-1} to 2700 cm^{-1} peak explanation

4.3 Melt Flow Index

Table 14 Melt flow index results

Sample		Average Mass	Melt flow index (g/10 min)	Observation
PP	Pure PP	Could not collect any sample	-	In first 60 seconds before applying the load materials started melting
	Reed (20%) + PP(80%)	0.1867 g	22.404	The test ran successfully, and five samples were collected
	NaOH treated reed (20%) + PP	0.2g Not valid (Only one sample was collected)	-	Material began to melt within the first 45 seconds, before applying the load
PLA	Pure PLA	0.64 g	12.8	Began melting before the load was applied (around 70 seconds), resulting in air bubbles during flow and touching the mirror surface in the MFI machine, which is considered a failure even though samples were counted successfully.
	Reed (20%) + PLA (80%)	Could not collect any sample	-	Significant darkening and a burnt smell, and was completely extruded within 60 seconds after load application, with the piston initially pushing upward.
	NaOH treated reed (20%) + PLA (80%)	Could not collect any sample	-	Large, uneven granules flowed out completely within 40 seconds of applying the load, with the piston even pushing outward at times
HDPE	Pure HDPE	Could not collect any sample	-	The HDPE granules started melting before applying the load, and no material was extruded after loading, making it impossible to cut any strands
	Reed (20%) + HDPE (80%)	0.1 g	12	Started melting at 38 seconds before the load was applied, and at around 80 seconds, the piston started rising upward.
	NaOH treated reed (20%) + HDPE (80%)	0.0675 g	8.1	Began flowing at 69 seconds before the load was applied, and the flow was smooth and easy to collect

4.3.1 Challenges in Sample Collection and Underlying Causes

- Pure PP

Two MFI tests were done using pure PP granules, with sample weights of 6.07 g and 8.06 g. The tests were run at 230 °C, and a 2.16 kg weight was added after 300 seconds of heating. In both cases, the PP started melting within the first minute, and material came out of the machine within the 360 seconds of a total time. According to the ASTM D1238 standard, the sample weights used were correct (within the recommended 4–8 g range). However, problems like air gaps in the sample, late application of the weight, or thick melt that couldn't flow might have caused the test to fail, even though the procedure followed the standard.

There are several possible reasons why no material came out during the MFI test, even though the samples melted. Even though the sample weights were within the standard 4–8 g range, the material might not have settled properly in the barrel, leaving air gaps or not fully covering the die, which can reduce pressure during the test. In many labs, using a slightly larger sample (9–10 g) helps avoid this. If PP had a lower melt flow rate than expected, was old or degraded, or had absorbed moisture, it might have been too thick to flow properly under normal test conditions(*Reinforcing PP with Natural Fibers*, n.d.; Sobczak et al., 2012).

- Reed (20%) + PP (80%)

The addition of natural fibers such as reed to PP typically results in a reduced MFI, which is an expected outcome. Reed fibers do not melt during processing; instead, they remain as solid particles within the polymer matrix. These solid inclusions act as physical barriers, increasing the overall viscosity of the melt and making it more difficult for the material to flow through the die during MFI testing. Moreover, surface interactions between the reed fibers and the polymer, especially when the fibers are rough or partially bonded to the matrix, contribute to additional internal resistance. As a result, while the unfilled PP may exhibit an MFI of 44 g/10 min, the composite containing 20% reed shows a significantly lower MFI of 22.4 g/10 min. This decrease reflects the combined flow behavior of both the polymer and the fiber filler, rather than that of the base polymer alone.

- NaOH treated reed (20%) + PP (80%)

The alkali treatment, if too strong or prolonged, can partially degrade the fiber structure, reducing the thermal stability of the composite and causing early softening or degradation during testing. While the alkali treatment improves mechanical bonding, it can also increase melt viscosity, making the composite more resistant to flow (Frącz et al., 2021). The use of a relatively low sample mass (4.9 g) might have also contributed to insufficient pressure build-up in the barrel, especially given the higher viscosity of the treated composite, leading to very limited material flow(Kabir et al., 2012).

- Pure HDPE

Pure HDPE failed to extrude any material, as the granules began melting before the load was applied and no strands could be collected after loading. This behavior may be attributed to several factors. One possibility is thermal instability or overheating, where the barrel temperature may have exceeded HDPE's optimal processing range, causing premature softening and increased viscosity. Inadequate compaction of the material or the presence of air gaps could also have disrupted pressure buildup inside the chamber, preventing the piston from pushing the melt effectively (ISO 1133, 2005).

- Reed (20%) + HDPE (80%)

The upward movement of the piston before applying the load was likely caused by internal pressure building up from the early melting of the composite. As the HDPE began to soften, it trapped air or moisture within the loosely packed or irregular composite granules. The presence of reed fibers, which are hydrophilic, may have contributed moisture that turned to steam during heating, further increasing the internal pressure. Since no downward force was yet applied, this pressure found the path of least resistance, pushing the piston upward(Kraiem et al., 2013b).

- NaOH treated reed (20%) + HDPE (80%)

Compared to pure HDPE, which melted too early and failed to give usable samples, the composite with alkali-treated reed behaved more predictably and allowed easy sampling. The presence of 20% alkali-treated reed fibers likely helped improve the composite's melt behavior by slightly increasing the melt viscosity and stabilizing the flow. The fibers may have acted as a structural support within the melt, preventing the kind of premature dripping or uncontrolled

flow seen in pure HDPE. Alkali treatment removes surface impurities and increases the interfacial bonding between the fibers and polymer matrix, leading to better thermal stability and more uniform heat distribution during melting(Kabir et al., 2012).

- Pure PLA

During the MFI test, the PLA sample started melting too early, before the load was applied which caused air bubbles to form and the material to drip down and touch the mirror. Also, since PLA flows quite easily when heated, any extra heat or poor temperature control in the machine could cause it to start flowing on its own, even without the applied load (Murariu & Dubois, 2016).

- PLA (80%) + reed (20%)

Reed can make PLA less stable at high temperatures and often contains moisture or natural materials that start to break down when heated. This can cause the material to burn, change color, and flow too quickly. If the composite was already overheated during injection moulding, it may have started degrading before the MFI test even began. During the test, the heat caused it to break down further, which explains the dark color and burnt smell. The piston pushing upward at first suggests that gases were forming inside, probably from moisture or early decomposition, creating pressure before the material started flowing. Once the load was applied, the entire sample rushed out in three quick bursts within 60 seconds, and the flow was so fast we couldn't collect any proper samples.

- PLA (80%) + NaOH reed (20%)

The fast flow and unusual piston movement during the test of the alkali-treated reed and PLA composite likely happened for a few reasons. The alkali treatment makes the reed surface rougher, which can help bonding but also makes it more likely to trap moisture or react differently under heat. That trapped moisture can turn into gas when heated, pushing the piston upward and making the material flow too quickly. Also, the granules in this batch were larger and uneven, which probably caused them to heat and melt at different rates. Some parts may have melted faster than others, leading to sudden bursts of flow. This uneven melting, along with possible early degradation, could explain why the whole sample rushed out within just 40 seconds and why the piston was being pushed up.

4.3.2 Comparison of the MFI values of treated and untreated fiber composites

HDPE was the only composite material that produced measurable MFI values for both treated and untreated fibers, making it the only candidate for comparison of fiber treatment effects.

The difference in MFI values, 12 g/10 min for the untreated reed + HDPE composite and 7.92 g/10 min for the NaOH-treated reed + HDPE compared to the much higher 25 g/10 min for pure HDPE, clearly shows how adding fibers and treating them affects how easily the material flows when melted. Adding untreated reed fibers already makes it harder for the molten HDPE to flow, since the rigid fibers get in the way and increase the material's resistance, reducing how much comes out during the test. When the reed is treated with NaOH, the flow slows down even more. This happens because the treatment improves the bond between the fibers and the HDPE, making the structure tighter and more cohesive. While both untreated and treated reed reduce the flow compared to pure HDPE, the treated version makes the composite behave in a more uniform and stable way, which explains the lower MFI.

5 Discussion

5.1 Alkali Treatment Challenges and Sample Preparation

The alkali treatment process, although essential for improving fiber-matrix bonding and removing amorphous components like lignin and hemicellulose, posed several logistical and technical challenges during this study. Using the available laboratory equipment, maintaining consistent conditions for soaking and rinsing required considerable time and effort. The five-hour soaking duration in NaOH solution and subsequent washing until neutral pH was labor-intensive, especially when processing larger batches. Furthermore, post-treatment grinding was necessary to achieve uniform fiber sizes for compounding, which introduced potential contamination risks. The grinding of treated samples may have allowed fragments of treated reed to mix inconsistently, potentially influencing the outcome of subsequent tests such as FTIR and optical microscopy. These limitations highlight the importance of streamlined processing protocols and the need for specialized equipment when working with treated lignocellulosic fibers.

5.2 Effects of Injection Molding and Micro-Compounding Parameters

In the fabrication of composite specimens, the use of micro-compounding and injection molding introduced complexities that potentially influenced the final properties of the Bio-composites. The PLA + reed composite samples appeared darker than expected, a phenomenon likely related to the elevated temperatures used (170–190 °C) and the possibility of residual materials within the compounder from earlier runs. Thermal degradation, particularly of PLA, may have occurred due to its sensitivity to heat and its tendency to retain moisture. In micro-compounding, previous material residues or insufficient cleaning may have led to cross-contamination. Additionally, the visual change in color of the PLA + reed composites could be partially attributed to changes in fiber surface chemistry during NaOH treatment, possibly exacerbated by uneven temperature distribution or residence time during processing.

5.3 FTIR Spectroscopy Considerations

FTIR spectroscopy was pivotal in identifying chemical modifications post-alkali treatment. However, a key challenge in this analysis was the inconsistency in sample sizes and

morphologies. Variability in fiber thickness, surface roughness, and particle distribution may have led to non-uniform pressure application during ATR measurement, affecting spectral clarity. Furthermore, the grinding of treated fibers could have introduced cross-contamination, where untreated or partially treated particles may have influenced spectral results. Notably, the presence of unusual peaks potentially associated with Si–O bonds suggests the influence of silicon-rich phytoliths in the common reed, a phenomenon that requires further investigation. These peaks may also result from the mineral content of the reed, accentuated by grinding and sample preparation procedures. This underlines the importance of preparing standardized samples for FTIR to ensure reliable comparison and interpretation.

5.4 Optical Microscopy Observations

The optical microscopy observations offered limited yet visually informative insights into the surface morphology of treated and untreated reed fiber composites. While alkali-treated samples appeared more uniform, with finer textures and seemingly better fiber dispersion, especially in PLA and PP matrices, these impressions are constrained to visible surface characteristics only. The method does not allow any conclusive interpretation regarding fiber-matrix bonding, internal structural integrity, or mechanical performance. Without quantitative image analysis or higher-resolution techniques, it is not possible to confirm whether visual improvements actually correlate with enhanced adhesion or functional properties. Additionally, from sample preparation, inconsistencies in sectioning using cutting blades or contamination carried over from prior experiments, may have influenced the appearance of surface features. The blades used to cut thin sections can introduce scratches, tears, or compressive deformations on the sample surface. Moreover, residues from earlier Micro-compounding or injection molding processes, such as uncleaned remnants of previous materials, may remain embedded in the composite and later appear in microscopy images. These factors can result in misleading visual cues, making it difficult to distinguish genuine morphological differences caused by alkali treatment. Optical microscopy cannot reveal subsurface defects, interfacial bonding strength, or the chemical state of the composite interfaces, making it difficult to draw any definitive conclusions beyond superficial observations. Therefore, while the visual data suggest potential improvements in composite morphology due to alkali treatment, the technique alone is insufficient for assessing the true extent or quality of bonding and internal structural changes.

5.5 Melt Flow Index (MFI) Results and Machine Limitations

MFI testing revealed critical processing behaviors of the polymer-reed composites but was limited by potential mismatches between machine specifications and composite flow characteristics. For instance, pure PP and PLA exhibited early melting or failed to extrude properly, possibly due to premature softening or trapped air. The composites, particularly those with NaOH-treated reed, displayed reduced MFI values, suggesting increased viscosity and fiber-matrix bonding strength. Notably, the HDPE + treated reed sample showed the most stable and measurable MFI performance, indicating that NaOH treatment contributed to more consistent and thermally stable flow behavior. However, for some formulations, the machine failed to collect consistent data due to backpressure effects, early flow, or excessive degradation. These inconsistencies highlight the potential inadequacy of standard MFI equipment for testing fiber-reinforced Bio-composites and underscore the need for method-specific calibration or modified protocols when working with natural fiber composites.

6 Conclusion

This research explored the effectiveness of sodium hydroxide (NaOH) treatment in enhancing the properties of common reed fibers for use in bio-composite applications. One major focus was to understand how this treatment influences the chemical composition and structure of the fibers. Through FTIR analysis, the treatment was shown to successfully remove amorphous components like hemicellulose and lignin, resulting in clearer, sharper peaks associated with crystalline cellulose. The visual transformation of the fiber surface, from smooth and waxy to rough and fibrillated, further confirmed structural modification. These changes aligned with expectations and demonstrated that alkali treatment substantially improves fiber compatibility with polymer matrices.

A key aim was to identify optimal conditions for enhancing crystallinity. While positive changes were observed, especially a sharper β-glycosidic cellulose peak indicating increased cellulose definition, the study was constrained by the use of a single treatment condition (4.5% NaOH for five hours). As such, while the treatment proved effective in general, the absence of variable testing meant that no optimal condition could be defined. This limits the precision of the conclusions and calls for a more expansive treatment matrix in future work.

Optical microscopy provided a basic qualitative overview of the surface morphology of treated and untreated reed fiber composites. While visual differences—such as smoother textures, reduced voids, and more uniform fiber dispersion—were observed in alkali-treated samples, especially in PP and PLA matrices, these findings are limited to surface-level interpretation. The technique does not offer sufficient resolution or depth to assess internal structural features, bonding quality, or mechanical integrity. Furthermore, potential artifacts introduced during sample cutting, and contamination from previous processing steps, may have influenced the visual output. As such, while the microscopy images suggest possible improvements in composite morphology due to alkali treatment, these observations remain inconclusive without support from more advanced analytical or mechanical characterization methods.

In terms of processing, MFI testing aimed to determine how treatment affected the ease of extrusion and mouldability of composites. This part of the study was only partially successful. While measurable reductions in MFI confirmed that treated fibers increased melt viscosity suggesting better interfacial bonding the testing was marred by equipment incompatibilities and inconsistent flow behaviors. Issues such as premature melting, trapped moisture, and piston

backflow, particularly in PLA and PP composites, led to poor sample collection and unreliable data in several cases. HDPE-based composites, however, offered the most consistent and usable results. These outcomes indicate that while NaOH treatment may improve fiber performance, it complicates processing conditions and requires more suitable testing setups for accurate flow analysis.

The thesis confirms that alkali treatment significantly improves the structural and interfacial behavior of reed fibers in thermoplastic composites. However, the lack of optimized treatment conditions and difficulties in flow testing limited the scope of measurable improvements. The study affirms the viability of *Phragmites australis* as a sustainable and functional fiber, while highlighting practical challenges in processing and testing fiber-reinforced composites.

6.1 Limitations

Several limitations impacted the depth and reproducibility of the findings. The NaOH treatment was applied using only one concentration and duration, limiting the ability to explore optimal conditions or treatment thresholds. Fiber processing introduced inconsistency in particle size and moisture content, affecting test uniformity especially in thermal and flow-sensitive experiments like MFI. Moisture retained in fibers likely led to premature melting, foaming, or degradation during heating, disrupting data collection. Equipment limitations, particularly the standard MFI machine not being suited for high-viscosity or fiber-filled samples, resulted in failed or invalid tests in multiple cases. Additionally, the presence of sample artifacts in microscopy and occasional spectral noise in FTIR hinted at issues in sample preparation and handling. For optical microscopy specifically, only surface features could be observed, with no capability to assess internal structure or bonding quality. Visual interpretation was further complicated by artifacts caused by cutting blades, uneven sectioning, and contamination from prior Micro-compounding or molding processes. These limitations restricted the ability to generalize certain outcomes or develop a robust process performance model.

6.2 Future Research Suggestions

To refine the insights gained in this thesis, future studies should systematically vary NaOH concentration, soaking duration, and treatment temperature to determine the most effective combination for fiber enhancement. This would help isolate the threshold beyond which fiber

degradation outweighs the benefits of treatment. Greater control over drying and storage conditions post-treatment is also essential to eliminate moisture-induced processing errors.

In terms of characterization, the use of TGA and DSC could provide deeper insights into thermal stability and degradation behavior post-treatment. Mechanical testing including tensile, flexural, and impact strength should be integrated to correlate fiber treatment with real-world performance metrics.

Regarding microscopy, future work should incorporate higher-resolution imaging techniques such as SEM to validate and expand upon the surface observations made through optical microscopy. This would allow detailed analysis of fiber-matrix interfaces, internal porosity, and failure mechanisms. Additionally, implementing image analysis software to quantify fiber dispersion and void content would enhance the objectivity of morphological evaluations and reduce reliance on subjective visual inspection.

7 References

Abou-Zeid, R. E., EL-Wakil, N. A., & Fahmy, Y. (2015). Thermoplastic Composites from Natural Reed Fibers. *Egypt. J. Chem.*, *3*.

Ágoston-Szabó, E., Dinka, M., Némedi, L., & Horváth, G. (2006). Decomposition of Phragmites australis rhizome in a shallow lake. *Aquatic Botany*, *85*(4), 309–316. https://doi.org/10.1016/j.aquabot.2006.06.005

Albrecht, K., Neudecker, F., Veigel, S., Bodner, S., Keckes, J., & Gindl-Altmutter, W. (2023). The suitability of common reed (Phragmites australis) for load-bearing structural materials. *Journal of Materials Science*, *58*(39), 15411–15420. https://doi.org/10.1007/s10853-023-08996-1

Amin, M. N., Ahmad, W., Khan, K., & Ahmad, A. (2022). A Comprehensive Review of Types, Properties, Treatment Methods and Application of Plant Fibers in Construction and Building Materials. *Materials*, *15*(12), 4362. https://doi.org/10.3390/ma15124362

Azka, M. A., Sapuan, S. M., Abral, H., Zainudin, E. S., & Aziz, F. A. (2024). An examination of recent research of water absorption behavior of natural fiber reinforced polylactic acid (PLA) composites: A review. *International Journal of Biological Macromolecules*, *268*, 131845. https://doi.org/10.1016/j.ijbiomac.2024.131845

Başaran Kankılıç, G., & Metin, A. Ü. (2020). Phragmites australis as a new cellulose source: Extraction, characterization and adsorption of methylene blue. *Journal of Molecular Liquids*, *312*, 113313. https://doi.org/10.1016/j.molliq.2020.113313

Brackhage, C., Schaller, J., Bäucker, E., & Dudel, E. G. (2013). Silicon Availability Affects the Stoichiometry and Content of Calcium and Micro Nutrients in the Leaves of Common Reed. *Silicon*, *5*(3), 199–204. https://doi.org/10.1007/s12633-013-9145-3

Carrillo, F., Colom, X., Suñol, J. J., & Saurina, J. (2004). Structural FTIR analysis and thermal characterisation of lyocell and viscose-type fibers. *European Polymer Journal*, *40*(9), 2229–2234. https://doi.org/10.1016/j.eurpolymj.2004.05.003

Dai, D., & Fan, M. (2011). Investigation of the dislocation of natural fibers by Fourier-transform infrared spectroscopy. *Vibrational Spectroscopy*, *55*(2), 300–306. https://doi.org/10.1016/j.vibspec.2010.12.009

Dallel, R., Kesraoui, A., & Seffen, M. (2018). Biosorption of cationic dye onto 'Phragmites australis' fibers: Characterization and mechanism. *Journal of Environmental Chemical Engineering*, *6*(6), 7247–7256. https://doi.org/10.1016/j.jece.2018.10.024

El Shahawy, A., & Heikal, G. (2018). Regression, kinetics and isotherm models for biosorption of organic pollutants, suspended and dissolved solids by environmentally friendly and economical dried *Phragmites australis*. *RSC Advances*, *8*(71), 40511–40528. https://doi.org/10.1039/C8RA07221C

Elenga, R. G., Djemia, P., Tingaud, D., Chauveau, T., Goma Maniongui, J., & Dirras, G. F. (2013). Effects of Alkali Treatment on the Microstructure, Composition, and Properties of the Raffia textilis Fiber. *BioResources*, *8*(2), 2934–2949. https://doi.org/10.15376/biores.8.2.2934-2949

Goswami, P., Blackburn, R. S., Taylor, J., & White, P. (2009). Dyeing behaviour of lyocell fabric: Effect of NaOH pre-treatment. *Cellulose*, *16*(3), 481–489. https://doi.org/10.1007/s10570-009-9279-z

Huhta, A. (2009). Decorative or Outrageous – The significance of the Common Reed (Phragmites australis) on water quality.

Jayamani, E., Loong, T. G., & Bakri, M. K. B. (2020). Comparative study of Fourier transform infrared spectroscopy (FTIR) analysis of natural fibers treated with

chemical, physical and biological methods. *Polymer Bulletin*, *77*(4), 1605–1629. https://doi.org/10.1007/s00289-019-02824-w

Kabir, M. M., Wang, H., Lau, K. T., & Cardona, F. (2012). Chemical treatments on plant-based natural fiber reinforced polymer composites: An overview. *Composites Part B: Engineering*, *43*(7), 2883–2892. https://doi.org/10.1016/j.compositesb.2012.04.053

Kanagaraj, S., Varanda, F. R., Zhil'tsova, T. V., Oliveira, M. S. A., & Simões, J. A. O. (2007). Mechanical properties of high density polyethylene/carbon nanotube composites. *Composites Science and Technology*, *67*(15–16), 3071–3077. https://doi.org/10.1016/j.compscitech.2007.04.024

Kavkler, K., Gunde-Cimerman, N., Zalar, P., & Demšar, A. (2011). FTIR spectroscopy of biodegraded historical textiles. *Polymer Degradation and Stability*, *96*(4), 574–580. https://doi.org/10.1016/j.polymdegradstab.2010.12.016

Khan, A., Sapuan, S. M., Yusuf, J., Siddiqui, V. U., Zainudin, E. S., Zuhri, M. Y. M., Tuah Baharuddin, B. T. H., Ansari, M. A., & Rahman, A. A. A. (2023). An examination of cutting-edge developments in Bamboo-PLA composite research: A comprehensive review. *Renewable and Sustainable Energy Reviews*, *188*, 113832. https://doi.org/10.1016/j.rser.2023.113832

Köbbing, J. F., Thevs, N., & Zerbe, S. (2013). *The utilisation of reed (Phragmites australis): A review*.

Kraiem, D., Pimbert, S., Ayadi, A., & Bradai, C. (2013a). Effect of low content reed (Phragmite australis) fibers on the mechanical properties of recycled HDPE composites. *Composites Part B: Engineering*, *44*(1), 368–374. https://doi.org/10.1016/j.compositesb.2012.04.062

Kraiem, D., Pimbert, S., Ayadi, A., & Bradai, C. (2013b). Effect of low content reed (Phragmite australis) fibers on the mechanical properties of recycled HDPE

composites. *Composites Part B: Engineering*, *44*(1), 368–374. https://doi.org/10.1016/j.compositesb.2012.04.062

Lei, Y., Wu, Q., Yao, F., & Xu, Y. (2007). Preparation and properties of recycled HDPE/natural fiber composites. *Composites Part A: Applied Science and Manufacturing*, *38*(7), 1664–1674. https://doi.org/10.1016/j.compositesa.2007.02.001

Li, Q., Ibrahim, L., Zhou, W., Zhang, M., & Yuan, Z. (2021). Treatment methods for plant fibers for use as reinforcement in cement-based materials. *Cellulose*, *28*(9), 5257–5268. https://doi.org/10.1007/s10570-021-03903-w

Madhavan Nampoothiri, K., Nair, N. R., & John, R. P. (2010). An overview of the recent developments in polylactide (PLA) research. *Bioresource Technology*, *101*(22), 8493–8501. https://doi.org/10.1016/j.biortech.2010.05.092

Murariu, M., & Dubois, P. (2016). PLA composites: From production to properties. *Advanced Drug Delivery Reviews*, *107*, 17–46. https://doi.org/10.1016/j.addr.2016.04.003

Ouajai, S., & Shanks, R. A. (2009). Preparation, structure and mechanical properties of all-hemp cellulose Bio-composites. *Composites Science and Technology*, *69*(13), 2119–2126. https://doi.org/10.1016/j.compscitech.2009.05.005

Pokhriyal, M., Rakesh, P. K., Rangappa, S. M., & Siengchin, S. (2024). Effect of alkali treatment on novel natural fiber extracted from Himalayacalamus falconeri culms for polymer composite applications. *Biomass Conversion and Biorefinery*, *14*(16), 18481–18497. https://doi.org/10.1007/s13399-023-03843-4

PP, UNIPOL Technology, Dow, Applications, Properties, Plastic, Polymer, Thermoplastic.

Qi, H., Wu, X., Chen, L., Liu, A., Deng, M., Wei, D., Wang, D., Peng, Z., & Wang, K. (2024). The Effect of Irradiation Combined with Sodium Hydroxide Pretreatment on Component, Structure, Utilization Efficiency of Phragmites Australis. *Waste and*

Biomass Valorization, *15*(12), 6615–6633. https://doi.org/10.1007/s12649-024-02571-8

Ray, D., Sarkar, B. K., Rana, A. K., & Bose, N. R. (2001). Effect of alkali treated jute fibers on composite properties. *Bulletin of Materials Science*, *24*(2), 129–135. https://doi.org/10.1007/BF02710089

Reinforcing PP with Natural Fibers. (2023)

Ren, Z., Wang, C., Zuo, Q., Siddique Yousfani, S. H., Anuar, N. I. S., Zakaria, S., & Liu, X. (2019). Effect of Alkali Treatment on Interfacial and Mechanical Properties of Kenaf Fiber Reinforced Epoxy Unidirectional Composites. *Sains Malaysiana*, *48*(1), 173–181. https://doi.org/10.17576/jsm-2019-4801-20

Sgriccia, N., Hawley, M. C., & Misra, M. (2008). Characterization of natural fiber surfaces and natural fiber composites. *Composites Part A: Applied Science and Manufacturing*, *39*(10), 1632–1637. https://doi.org/10.1016/j.compositesa.2008.07.007

Skrifvars, S. M., & Arya, M. (2023). *Hemp shives composites internship report*.

Sobczak, L., Lang, R. W., & Haider, A. (2012). PP composites with natural fibers and wood – General mechanical property profiles. *Composites Science and Technology*, *72*(5), 550–557. https://doi.org/10.1016/j.compscitech.2011.12.013

Suárez, L., Ortega, Z., Romero, F., Paz, R., & Marrero, M. D. (2022). Influence of Giant Reed Fibers on Mechanical, Thermal, and Disintegration Behavior of Rotomolded PLA and PE Composites. *Journal of Polymers and the Environment*, *30*(11), 4848–4862. https://doi.org/10.1007/s10924-022-02542-x

Uzatici, A., Canbolat, O., & Kamalak, A. (2022). Effect of Sodium Hydroxide Treatment on Chemical Composition and Feed Value of Common Reed (Phragmites australis) Straw. *Fermentation*, *8*(12), 749. https://doi.org/10.3390/fermentation8120749

Varshney, D., Debnath, K., & Singh, I. (2014). *Mechanical Characterization of PP (PP) and Polyethylene (PE) Based Natural Fiber Reinforced Composites*.

Wang, X., Deng, Y., Wang, S., Liao, C., Meng, Y., & Pham, T. (2013b). Nanoscale Characterization of Reed Stalk Fiber Cell Walls. *BioResources*, *8*(2), 1986–1996. https://doi.org/10.15376/biores.8.2.1986-1996

Wöhler-Geske, A., Moschner, C. R., & Gellerich, A. (2016). Provenances and properties of thatching reed (Phragmites australis). *Landbauforschung - Applied Agricultural and Forestry Research*, *66/1*, 1–10. https://doi.org/10.3220/LBF1457686750000

DSM Xplore. (2016). *Micro-compounder / Extruder 15 ml*.

ISO 1133: Melt flow index (MFI) plastics. (2005). ISO 1133: Melt Flow Index (MFI) Plastics. https://www.zwickroell.com/industries/plastics/thermoplastics-and-thermosetting-molding-materials/melt-flow-index-test-iso-1133/

Linderbäck, P., Gebrehiwot, S., Montin, L., Björkvall, R., Suarez, L., Theis, J., & Z. Ortega. (2024). common reed as a novel biosource for composite production. In *ECCM21 – 21st European Conference on Composite Materials*. ECCM21 – 21st European Conference on Composite Materials. https://www.researchgate.net/publication/382108396

Plastics — Determination of the melt mass-flow rate (MFR) and the melt volume-flow rate (MVR) of thermoplastics. (2005). https://standards.iteh.ai/catalog/standards/sist/a41e52b7-9043-492f-a5c0-c9aa9baa7bf5/iso-1133-2005

Suárez, L., Billham, M., Garrett, G., Cunningham, E., Marrero, M. D., & Ortega, Z. (2023). A new image analysis assisted Semi-Automatic Geometrical measurement of fibers in thermoplastic composites: a case study on giant Reed fibers. *Journal of Composites Science*, *7*(8), 326. https://doi.org/10.3390/jcs7080326

Thermo Fisher Scientific Inc. (2019). *Thermo Scientific Process 11 Twin-screw extruder*. https://thermofisher.com/process11

Thermo Fisher Scientific Inc. (2021). *Nicolet Summit FTIR Spectrometer User Guide*. https://assets.thermofisher.com/TFS-Assets/MSD/Product-Information/Summit-UG.pdf

Xplore Instruments BV. (2021). *Xplore IM12*. https://www.xplore-together.com

A-MELT NOSELAB ATS s.r.l. https://www.noselab-ats.com/en/products/plastic-and-rubber-testing/raw-material-characterisation/a-melt/

Axio Scope.A1 - LABORSCIENCE A.E. (2017, November 9). LABORSCIENCE A.E. https://www.laborscience.com.gr/product/axio-scope-a1/

Fct/Unl *Xplore Micro-compounder 5 | CENIMAT*. https://www.cenimat.fct.unl.pt/services/laboratory-electronic-and-optoelectronic-materials-and-devices/xplore-micro-compounder-5-0

Güven, O., Monteiro, S. N., Moura, E. a. B., & Drelich, J. W. (2016). Re-Emerging Field of Lignocellulosic Fiber – Polymer Composites and Ionizing Radiation Technology in their Formulation. *Polymer Reviews*, *56*(4), 702–736. https://doi.org/10.1080/15583724.2016.1176037

Hooshmand, S., Aitomäki, Y., Skrifvars, M., Mathew, A. P., & Oksman, K. (2014). All-cellulose nanocomposite fibers produced by melt spinning cellulose acetate butyrate and cellulose nanocrystals. *Cellulose*, *21*(4), 2665–2678. https://doi.org/10.1007/s10570-014-0269-4

Carl Zeiss MicroImaging GmbH. (2008). *Operating Manual Axio Scope.A1 Microscope for Routine and Entry-Level research* (No. M60-2-0007 e). https://www.zeiss.de

Frącz, W., Janowski, G., & Bąk, Ł. (2021). Influence of the alkali treatment of flax and hemp fibers on the properties of PHBV based biocomposites. *Polymers*, *13*(12), 1965. https://doi.org/10.3390/polym13121965

Smith, B. C. (2024). Infrared Spectral Interpretation, In the beginning i: The meaning of peak positions, heights, and widths. *Spectroscopy*, 18–24. https://doi.org/10.56530/spectroscopy.fi6379n1

Xie, Y., Hill, C. A. S., Xiao, Z., Militz, H., Mai, C., Wood Biology and Wood Products, Burckhardt-Institute, Georg August University of Göttingen, Büsgenweg 4, D37077 Göttingen, Germany, & Centre for Timber Engineering, School of Engineering and the Built Environment, Edinburgh Napier University, 10 Colinton Road, EH10 5DT Edinburgh, United Kingdom. (2010). Silane coupling agents used for natural fiber/polymer composites: A review. In *Composites: Part A* (Vol. 41, pp. 806–819) [Journal-article]. https://doi.org/10.1016/j.compositesa.2010.03.005

Kaysar, M. A., Ahmed, S. J., Jamil, A. T. M. K., Habib, M. M., Dayan, M. a. R., Mamun-Or-Rashid, N., & Gafur, M. A. (2024). Impact of NAOH treatment on the chemical, structural, physico-mechanical, and thermal characteristics of jute species. *Fibers and Polymers*, *25*(5), 1765–1777. https://doi.org/10.1007/s12221-024-00542-3

Lavorel, F., Mansori, M. E., Chegdani, F., & Tazibt, A. (2021). Wear under brittle removal regime of an under-expanded cryogenic nitrogen jet machining of bio-composites. *Wear*, *477*, 203795. https://doi.org/10.1016/j.wear.2021.203795

Williams, T., Hosur, M., Theodore, M., Netravali, A., Rangari, V., & Jeelani, S. (2011). Time effects on morphology and bonding ability in mercerized natural fibers for composite reinforcement. *International Journal of Polymer Science*, *2011*, 1–9. https://doi.org/10.1155/2011/192865

Xia, T., Huang, H., Wu, G., Jin, X., Sun, E., & Tang, W. (2017). Study on the Acetylation of Rice Straw-Biogas Residue and its Characteristic Effect on Rice Straw-Reinforced Composites. *BioResources*, *12*(3). https://doi.org/10.15376/biores.12.3.5736-5748

Xplore Instruments. (2019, November 5). *Using an IM 12 micro injector with a Xplore Micro-compounder* [Video]. YouTube. https://www.youtube.com/watch?v=-H0DtptBA9o

Yadav, V. K., Verma, N., Kardam, S. K., & Pullela, M. (2025). Pineapple Leaf Fiber in Polymer Composites: Structure, Characterization, and Applications. *Materials Chemistry and Physics.*, 100011. https://doi.org/10.1016/j.macse.2025.100011

Yasuda seiki seisakusho, ltd. (2025, May 12). *What is Melt Mass-Flow Rate (MFR) and Melt Volume-Flow Rate (MVR)? | Yasuda seiki seisakusho, ltd.* Yasuda seiki seisakusho, ltd. | yasuda seiki seisakusho, ltd. https://yasudaseiki.com/what-is-mfr-and-mvr/

Data Sheet C705-44NA HP. (2019).

Mohanty, A. K., Misra, M., & Drzal, L. T. (2001). Surface modifications of natural fibers and performance of the resulting biocomposites: An overview. *Composite Interfaces*, *8*(5), 313–343. https://doi.org/10.1163/156855401753255422

The Lake Huron Centre for Coastal Conservation. (2006). Invasive species in coastal areas. In *The Lake Huron Centre for Coastal Conservation*. https://www.lakehuron.on.ca

Alcock, B., Cabrera, N. O., N.-M. Barkoula, Loos, J., Peijs, T., Department of Materials, Queen Mary University of London, & Eindhoven Polymer Laboratories, Eindhoven University of Technology. (2005). The mechanical properties of unidirectional all-polypropylene composites. In *Composites: Part A* (Vol. 37, pp. 716–726) [Journal-article]. Elsevier Ltd. https://doi.org/10.1016/j.compositesa.2005.07.002

Hinchcliffe, S. A., Hess, K. M., & Srubar, W. V. (2016). Experimental and theoretical investigation of prestressed natural fiber-reinforced polylactic acid (PLA) composite

materials. *Composites Part B Engineering*, *95*, 346–354. https://doi.org/10.1016/j.compositesb.2016.03.089

Zhang, S., Cao, X. Y., M, Y., MA, Ke, Y. C., Zhang, J. K., & Wang, F. S. (2011). The effects of particle size and content on the thermal conductivity and mechanical properties of Al2O3/high density polyethylene (HDPE) composites. *eXPRESS Polymer Letters*, *5*(7), 581–590. https://doi.org/10.3144/expresspolymlett.2011.57